SD95-20-F

Department of Transportation
Office of Research

Thickness Design for Jointed Fiber Reinforced Concrete Highway and Street Pavements

Study SD95-20
Final Report

Prepared by
Yongxin Liu
South Dakota Department of Transportation
700 E Broadway Avenue
Pierre, SD 57501

September 1995

DISCLAIMER

The contents of this report reflect the views of the authors who are responsible for the facts and accuracy of the data presented herein. The contents do not necessarily reflect the official views or policies of the South Dakota Department of Transportation, the State Transportation Commission, or the Federal Highway Administration. This report does not constitute a standard, specification, or regulation.

ACKNOWLEDGEMENTS

This work was performed under the supervision of the SD95-20 Technical Panel:

Don Anderson . . . . . Materials & Surfacing
Toby Crow . . . . . Planning & Programs
Ron McMahon . . . Office Materials & Testing
Cliff MacDonald . . . . . 3M Corporation
Paul Nelson . . . . . Office of Bridge Design
Dwight Pogany . . . . . Pierre Area
Jim Sanders . . . . . 3M Corporation
Ariel Soriano . . . . . Office of Research
Ginger Massie . . . . . FHWA
Daniel Strand . . . . . Office of Research

The contribution of Professor V. Ramakrishnan (Dept. of Civil Engineering, South Dakota School of Mines and Technology) is gratefully acknowledged.

TECHNICAL REPORT STANDARD TITLE PAGE

1. Report No.	2. Government Accession No.	3. Recipient's Catalog No.
SD95-20-F		

4. Title and Subtitle	5. Report Date
Thickness Design for Jointed Fiber Reinforced Concrete Highway and Street Pavements	August 31, 1995
	6. Performing Organization Code

7. Author(s)	8. Performing Organization Report No.
Yongxin Liu	

9. Performing Organization Name and Address	10. Work Unit No.
South Dakota Department of Transportation 700 East Broadway Avenue Pierre, SD 57501-2586	11. Contract or Grant No.

2. Sponsoring Agency Name and Address	13. Type of Report and Period Covered
South Dakota Department of Transportation Office of Research 700 East Broadway Avenue Pierre, SD 57501-2586	Final; Feb. 1995 to Sept. 1995
	14. Sponsoring Agency Code

15. Supplementary Notes

16. Abstract

A thickness design method for jointed fiber reinforced concrete pavements is developed by modifying the current PCA "Thickness Design for Concrete Highway and Street Pavements" based on the fact that the fatigue properties of fiber reinforced concrete (FRC) are different from those assumed in the design procedure for conventional concrete pavements. To recognize the unique fatigue properties of FRC, new endurance limit and fatigue S-N curves (Fatigue Stress Ratio versus Number of Load Repetitions) must be established from test data of the FRC. It is impractical or impossible to develop a uniform endurance limit and S-N function for all kinds of FRC because the fatigue properties of FRC vary significantly with fiber type, fiber content, aspect ratio, bonding and anchorage features, and mix design. However, an evaluation of steel fiber reinforced concrete pavements in field application (Haines Avenue in Rapid City, South Dakota) demonstrates how the fatigue properties of a specific FRC are determined and used in the modified thickness design method.

Both the theoretical analysis and the field inspection indicate that the steel fiber reinforced concrete pavement is very strong against transverse fatigue cracking. On the other hand, the deflection at joints becomes the major concern of FRC pavement design because of reduced thickness and increased flexibility. The PCA erosion criterion, which is derived from critical deflection and subbase pressure near joints, provides a useful control over erosion and other distresses in association with slab joints.

17. Keyword	18. Distribution Statement
	No restrictions. This document is available to the public from the sponsoring agency.

19. Security Classification (of this report)	Security Classification (of this page)	21. No. of Pages	22. Price
Unclassified	Unclassified	88	

TABLE OF CONTENTS

LIST OF TABLES

LIST OF FIGURES

GLOSSARY

Terms

Aspect Ratio - The ratio of length to diameter of the fiber. Diameter may be equivalent diameter.

Endurance limit - The fatigue stress level at which the concrete beams tested can withstand two-million cycles of non-reversed fatigue loading, expressed as a percentage of the static flexural strength.

Equivalent Diameter - Diameter of a circle with an area equal to the cross-sectional area of the fiber.

Fiber Content - The weight of fibers in a unit volume of concrete.

Fatigue Stress - The extreme bending stress under repetitive loading.

Fatigue Stress Ratio - The ratio of fatigue stress to static flexural strength.

Fatigue S-N Curve or S-N Curve - The curve presenting a function of fatigue stress ratio and number of load repetitions.

First Crack - The point on the flexural load-deflection curve at which the form of the curve first becomes nonlinear.

First Crack Deflection - The deflection value on the load deflection curve at the first crack.

First Crack Strength - The stress obtained when the load corresponding to the first crack is inserted in the formula for modulus of rupture given in ASTM Test Method C78.

Flexural Toughness - The area under the flexural load-deflection curve obtained from a static test of a specimen up to a specified deflection. It is an indication of the energy absorption capacity of a material.

Modulus of Rupture - The static flexural strength of concrete determined in accordance with ASTM C78.

Static Modulus - the value of Young's modulus of elasticity obtained from measuring stress-strain relationships under static loading.

Toughness Indices - The number obtained by dividing the area under the load-deflection curve up to a specified deflection by the area under the load-deflection curve up to the first crack.

Toughness Index, I_5 - The number obtained by dividing the area up to 3.0 times the first crack deflection by the area up to the first crack of the load deflection curve.

Toughness Index, I_{10} - The number obtained by dividing the area up to 5.5 times the first crack deflection by the area up to the first crack of the load deflection curve.

Toughness Index, I_{20} - The number obtained by dividing the area up to 10.5 times the first crack deflection by the area up to the first crack of the load deflection curve.

Abbreviations

AASHO - American Association of State Highway Officials

AASHTO - American Association of State Highway and Transportation Officials

ACI - American Concrete Institute

ADT - Average daily traffic in both directions (all vehicles)

ADTT - Average daily truck traffic in both directions (excluding two-axle, four-tire trucks)

ASTM - American Society for Testing and Materials

CRCP - Continuous reinforced concrete pavement

JPCP - Jointed plain concrete pavement

LSF - Load safety factor

FRC - Fiber reinforced concrete

FHWA - Federal Highway Administration

PCA - Portland Cement Association

PCC - Portland cement concrete

SD DOT - South Dakota Department of Transportation

SFRC - Steel fiber reinforced concrete

Standards and Specifications

ACI 544.2R. - Measurement of Properties of Fiber Reinforced Concrete

ACI 544.3R. - Guide for Specifying, Proportioning, Mixing, Placing, and Finishing Steel Fiber Reinforced Concrete

ASTM A820 - Specification for Steel Fibers for Fiber Reinforced Concrete

ASTM C31 - Practices for Making and Curing Concrete Test Specimens in the Field

ASTM C33 - Specification for Concrete Aggregates

ASTM C39 - Test Method for Compressive Strength of Cylindrical Concrete Specimens

ASTM C78 - Test Method for Flexural Strength of Concrete (Using Simple Beam with Third-Point Loading)

ASTM C150 - Specification for Portland Cement

ASTM C231 - Test Method for Air Content of Freshly Mixed Concrete by the Pressure Method

ASTM C469 - Test method for Static Modulus of Elasticity and Poisson's Ratio of Concrete in Compression

ASTM C618 - Specification for Fly Ash and Raw or Calcined Natural Pozzolan for Use as a Mineral Admixture in Portland Cement concrete.

ASTM C1018 - Test Method for Flexural Toughness and First Crack Strength of Fiber Reinforced Concrete (Using Beam with Third-Point Loading)

Notations

a	=	Radius of contact area
A,B,C	=	Constants or coefficients
C_d	=	Drainage coefficient
CV	=	Coefficient of variation
D_r	=	The fatigue damage ratio accumulated over the design period due to all groups of traffic loads

E	=	Elastic modulus of concrete
F	=	The wheel load
F_A	=	Ratio of the modulus of rupture at time T to the modulus of rupture at 28 days
h	=	The thickness of the slab
J	=	Load transfer coefficient used to adjust for the load transfer characteristics of a specific design
k	=	The modulus of subgrade reaction
l	=	Radius of relative stiffness
m	=	The total number of load groups
MR	=	Modulus of rupture
MR_{28}	=	Mean modulus of rupture at 28 days
MR_{60}	=	Mean modulus of rupture at 60 days
MR_{28d}	=	Design modulus of rupture at 28 days
n_i	=	The predicted number of repetitions in the design period for the *i*th load group
N	=	Number of load applications
N_i	=	The allowable number of repetitions for *i*th load group
N_d	=	The allowable number of load applications for pavement design
P	=	Power with which an axle load deflects the slab
P_i	=	Initial serviceability
P_t	=	Terminal serviceability
p	=	Pressure under the slab
S_o	=	Overall standard deviation for rigid pavement

S_c = Static flexural strength of concrete (It can be different from modulus of rupture determined by ASTM C78 when the variation in concrete strength and the strength gain with age are considered.)

T = Time since slab construction in years

W_{18} = Predicted number of 18-kip (80-kN) equivalent single axle load applications,

Z_R = Standard normal deviation corresponding to selected level of reliability

ν = Poisson's ratio of concrete

σ = Fatigue stress

σ_c = The maximum bending stress due to corner loading

σ_e = The maximum bending stress due to edge loading

σ_i = The maximum bending stress due to interior loading

1. INTRODUCTION

Tasks 1& 2: The tasks of this chapter are to state the problem, review the literature in rigid pavement design, and summarize the current jointed concrete pavement design theories and design methods. The material presented provides insight into the fatigue design criterion, erosion design criterion (PCA design method), and how they are used in the current design procedures.

1.1 Problem Statement

Significant improvement in mechanical properties of tension-weak concrete can be achieved by the incorporation of fibers. These properties include static flexural strength, flexural fatigue strength, flexural toughness, ductility, and impact strength. Continuing research, product development and marketing are steering the application of fiber reinforced concrete (FRC). Numerous papers on the topic are published every year; new fiber products made of different materials and in different shapes are emerging; and many FRC pavements have been built in the USA on streets, highways and airports in the last 20 years [29]. For pavement structures, the major benefit from fiber reinforcement is its ability to prevent fatigue cracking which is a principle distress in concrete pavements. Most current mechanistic design methods use flexural strength and fatigue strength of plain concrete as the basic material design factors for plain concrete pavement design because they are directly related to the actual pavement performance. For FRC pavements, the fatigue property has been improved and the existing design methods have to be modified to reflect the change. How the other material properties of plain concrete or FRC (flexural toughness, ductility, and impact strength) affect pavement performance and how they should be used in the pavement design are unknown.

1.2 Literature Review

Pavement design has gradually evolved from art to science. Prior to the early 1920s, the thickness of pavement was based purely on experience. As experience was gained throughout the years, various analysis theories and design methods were developed by different agencies for determining the thickness of Portland cement concrete (PCC) pavements. Both mechanistic design procedures based on analytical solutions and empirical design methods based on pavement performance in road tests have been used. The current trend is to combine the two with the help of computer technology which can give sophisticated finite element solutions and statistical analyses of pavement performance data.

1.2.1 Analytical Solutions

Methods from simple formulas to complex derivations are available for determining the stresses and deflections in concrete pavements.

Goldbeck's Formula

By assuming the pavement as a cantilever beam with a concentrated load acting at the corner, Goldbeck (1919) developed a simple equation for the design of rigid pavement [15]:

$$\sigma_c = 3F/h^2 \qquad (1.1)$$

where σ_c = the maximum bending stress due to corner loading,

F = the concentrated wheel load,

h = the thickness of the slab.

The same equation was applied by Older (1924) in the Bates Road Test [22].

Westergaard's Analysis Based on Liquid Foundations

The most extensive theoretical studies on the stresses and deflections in concrete pavements were made by Westergaard [37], who developed equations for three cases of loading: load applied near the corner of a large slab, load applied near the edge of a large slab but at a considerable distance from any corner, and load applied at the interior of a large slab at a considerable distance from any edge. The analysis was based on the assumption that the reactive pressure between the slab and the subbase at any given point is proportional to the deflection at that point, independent of the deflections at any other points. This type of foundation is called a liquid foundation or Winkler foundation. The load was applied on a circle (radius = a). The equations are given as follows:

Corner Loading: $$\sigma_c = (3F/h^2)[1-(2^{0.5}\, a/\, l\,)^{0.6}] \quad (1.2)$$

where l = radius of relative stiffness defined as:

$$l = \{(Eh^3)/[12k(1-\nu^2)]\}^{0.25} \quad (1.3)$$

where E = elastic modulus of concrete,

ν = Poisson's ratio of concrete,

k = the modulus of subgrade reaction.

Edge Loading: $$\sigma_e = [3(1+\nu)F/\pi(3+\nu)h^2][\ln(Eh^3/100ka^4) + 1.84 - 4\nu/3 + (1-\nu)/2 + 1.18a(1+2\nu)/l] \quad (1.4)$$

Interior Loading: $\sigma_i = [3F(1+v)/2\pi h^2][\ln(l/B) + 0.6519]$ (1.5)

where $B = a$, when $a \geq 1.72h$

$B = (1.6a^2 + h^2)^{0.5} - 0.675h$, when $a \leq 1.724h$

Pickett's Analysis on Solid Foundations

In view of the fact that the actual subgrade behaved more like an elastic solid than a dense liquid, Pikett et al. developed theoretical solutions for concrete slabs on an elastic half space and a simple influence chart based on solid foundations for determining the edge stresses [28].

1. 2. 2 Finite Element Solutions

With the development of the powerful finite element method, a breakthrough was made in the analysis of rigid pavements. There are numerous computer programs available such as JSLAB, ILLISLAB, KENSLABS, WESTLIQUID, WESTLAYER, CRCP-2, RISC, just to name a few. Heinrichs [16] compared several computer models for rigid pavements and concluded that both JSLAB [36] and ILLISLAB [35] were efficient to use. The programs allows considerations of slabs with finite dimensions, variable axle-load placement, and modeling of load transfer at transverse joints or at the joint between pavement and concrete shoulder. For doweled joints, dowel properties such as diameter and modulus of dowel-concrete reaction are used directly. For aggregate interlock, a shear spring stiffness constant is used to present the load-deflection characteristics of such joints. The programs can calculate many key structural design factors such as critical stresses and critical deflections.

Assumptions in the development of JSLAB and ILLISLAB are identical and summarized as follows:

1. Small deformation theory of an elastic, homogeneous medium-thick plate is employed for the concrete slab, stabilized base and overlay. Such a plate is thick enough to carry transverse load by flexure, rather than in-plane force (as would be the case for a thin member), yet is not so thick that transverse shear deformation becomes important.

2. In the case of a bonded stabilized base or overlay, full strain compatibility is assumed at the interface. For the unbonded case, shear stresses at the interface are neglected.

3. When aggregate interlock is specified for load transfer, load is transferred from one slab to an adjacent slab by shear. However, with dowel bars some moment as well as shear may be transferred across joints.

4. Dowel bars at joints are linearly elastic, and are located at the neutral axis of the slab.

5. Three different types of foundations can be assumed: liquid, solid, and layer. Only two layers can be used in layer foundation.

The stiffness matrix in both JSLAB and ILLISLAB for the subgrade considered is based on the work of Tabatabaie [34]. As expected, both programs yield practically the same results. There are some technical differences between the two programs in calculation procedures, and some details of input and output. For example, JSLAB output provides nodal bending stresses along X and Y axes; ILLISLASB prints out

nodal principal stresses.

The input of program JSLAB includes: 1) Geometry of the slab or slabs, and mesh configuration. 2) Load transfer system at the joints. 3) Elastic properties and thickness of PCC slab, stabilized base or overlay. 4) Subgrade stiffness. 5) Unit weight of concrete and temperature gradient through slab. 6) Initial slab displacements (if not zero). 7) Applied loads. The output produced by JSLAB includes: 1) Dowel shear and moment at each node along joint. 2) Nodal deflections and rotations. 3) Nodal bending stresses along X and Y axes. 4) Nodal shear stresses in XY plane. 5) Nodal vertical component of applied load. 6) Nodal moment component of applied load along X and Y axes.

1. 2. 3 Design Criteria

Structural analysis of rigid PCC pavements with an output of critical stresses and deflections under given static loads is only one part of pavement design. Street and highway pavements are subjected to repetitive traffic loads over a design period. Design is not simply a matter of applying static loads one time. The concrete static flexural strength (modulus of rupture) can not be directly compared with the stresses calculated by finite element methods without considering the frequency of loading, different axle-distributions of the truck traffic, and design life. The design criteria must also be related to major types of distress of jointed concrete pavements such as fatigue cracking and erosion.

Fatigue

Fatigue is a process of progressive, permanent internal damage in a structure subjected to repetitive loading. Fatigue cracking is one of the principle distresses in PCC pavement. An extensive study was made by the Illinois Division of Highways during the Bates Road Test on the fatigue properties of plain concrete [12]. It was found that if the intensity of extreme bending stress did not exceed approximately 50 % of the modulus of rupture, the flexural stress could be repeated indefinitely without causing rupture, and that, if the stress ratio was above 50 %, the allowable number of stress repetitions to cause failures decreased drastically as the stress ratio increased. Although the arbitrary use of 50 % stress ratio as a dividing line was not actually proved, the latter research [13] revealed that the average fatigue strength of plain concrete under two million cycles is about 50 % to 55% of its static flexural strength. Because of the logarithmic nature of the function, little loss in fatigue strength actually occurs with continued repetitions of loads after two million cycles. The 50 % stress ratio has been used most frequently in later mechanistic design methods. To obtain a smoother fatigue curve, the current PCA method assumed a stress ratio of 45% [25], below which no fatigue damage need be considered. The fatigue design factors are endurance limit, S-N function, critical fatigue location in slab, and traffic data in design period. A cumulative fatigue damage theory is used for the final judgement of fatigue failure.

Endurance Limit

The endurance limit of concrete, as defined in this report, is the fatigue stress level at which the concrete beams tested can withstand two million cycles of non-reversed

fatigue loading, expressed as a percentage of its static flexural strength [4]. Adding steel fibers in concrete can significantly improve fatigue properties. Steel fiber reinforced concrete (SFRC) has endurance limits ranging from 55% to 90% depending on quality and quantity of fibers used and the properties of the concrete mix [3,5,20].

S-N Curve

When the fatigue stress due to applied loads is greater than the endurance limit, the allowable number of repetitions is a function of the fatigue stress, usually expressed as a ratio of the fatigue stress to the static flexural strength. The classical approach to fatigue design has focused on establishment of the S-N function. The number of repetitions can be predicted by an equation:

$$\log N = A - B\,(\sigma/S_c) \qquad (1.6)$$

where N = number of load applications,

S_c = static flexural strength of concrete,

σ = fatigue stress,

A and B = coefficients determined from fatigue test data.

Fatigue data of plain concrete beams from three studies were processed and a regression curve was fit to the data base, which produced A = 17.61, B = 17.61 [13]:

$$\log N = 17.61 - 17.61\,(\sigma/S_c) \qquad (1.7)$$

This equation is a mean regression curve which presents a failure probability of 50 percent. A design equation usually uses a smaller allowable number of repetitions to lower the probability of failure. In the "Design of Zero-Maintenance Plain Jointed

Concrete Pavement", Darter and Barenberg [13] recommended a reduction by one order of magnitude. The design curve (Eq. 1.8) presents a failure probability of 24 percent:

$$\log N_d = 16.61 - 17.61\ (\sigma/S_c) \qquad (1.8)$$

The fatigue S-N equations recommended by the PCA Thickness Design Method are expressed as Eq. 1.9a through 1.9c [25]. These equations were developed on a similar test data base but a much lower failure probability was used (The actual failure probability is not given but the graphic curve of PCA equations shows that it is lower than the 5 % failure probability curve established by Hilsdorf and Kesler [13]).

For $(\sigma/S_c) \geq 0.55$: $\log N_d = 11.737 - 12.077\ (\sigma/S_c)$ (1.9a)

For $0.45 < (\sigma/S_c) < 0.55$: $N_d = \{4.2577 / [(\sigma/S_c)-0.4325]\}^{3.268}$ (1.9b)

For $(\sigma/S_c) \leq 0.45$: N_d = unlimited (1.9c)

Fatigue Criterion and Miner's Damage Hypothesis

The classic hypothesis for determining the degree of fatigue damage due to random stresses is Miner's hypothesis, which assumes that fatigue resistance not consumed by repetitions of one group of loads is available for repetitions of other groups of loads.

$$D_r = \sum_{i=1}^{m} (n_i / N_i) \qquad (1.10)$$

Where D_r is the damage ratio accumulated over the design period due to all groups of traffic loads, m is the total number of load groups, n_i is the predicted number of repetitions in the design period for the *i*th load group, and N_i is the allowable number of repetitions for *i*th load group, which can be determined from Eqs. 1.9a through

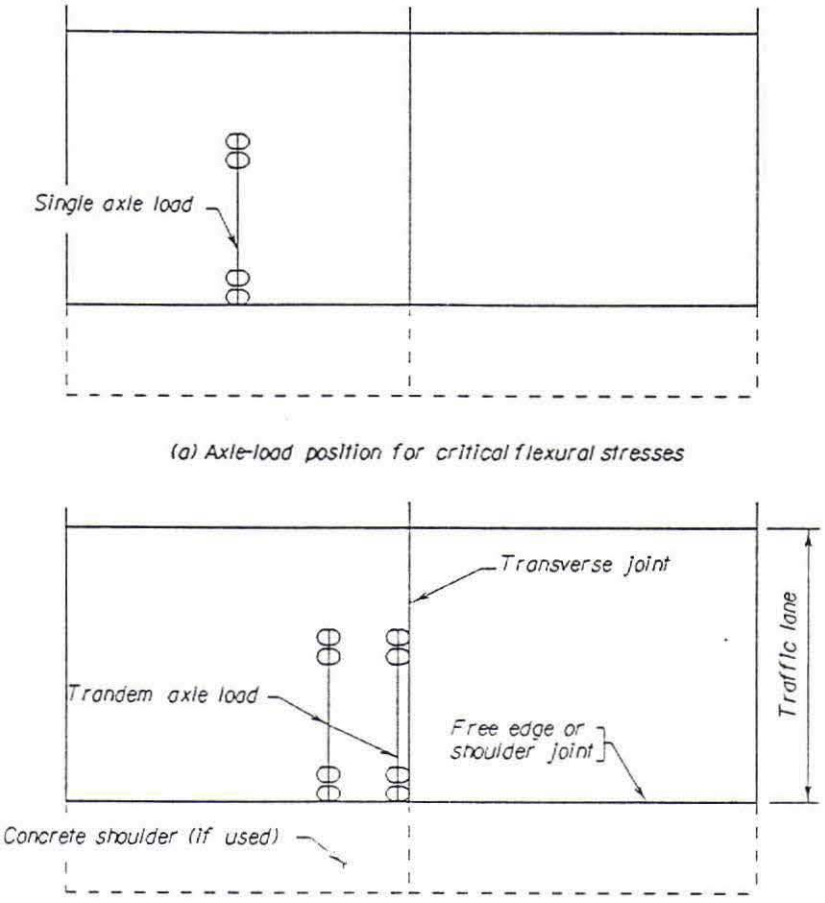

Figure I.1 Critical Axle Load Positions.

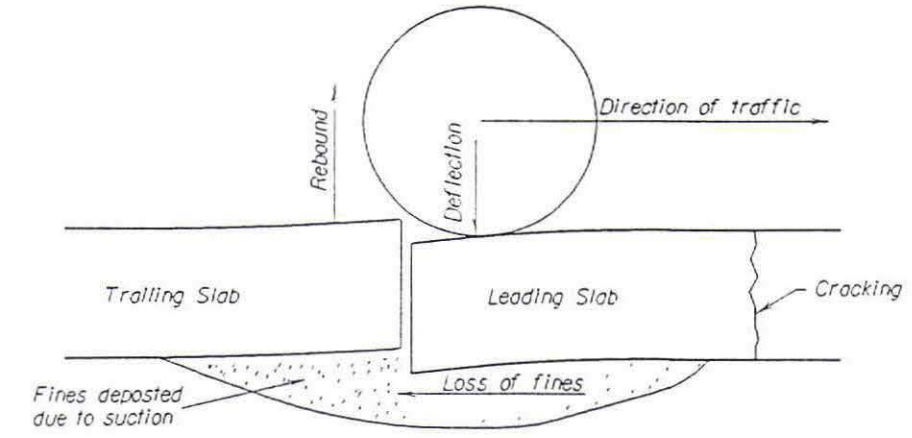

Figure I.2 Pumping of Rigid Pavement.

1.9c for PCA method or from Eq. 1.8 for the Design of Zero-Maintenance Plain Jointed Concrete Pavements.

The fatigue design criterion is based on both the S-N curve established from the tested data and the damage ratio. The PCA method, which is conservative in Eqs. 1.9a through 1.9c, requires that the accumulated damage ratio at the end of the design period should be smaller than 1.0 [25]. The Design of Zero-Maintenance Pavement method, which is not so conservative in its S-N equation, sets the limit of the accumulated damage ratio not greater than 0.0001 [13].

Critical Fatigue Location in Slab and Truck Load Placement

Location of the critical point at which cracking initiates in the PCC slab is vital to the development of a fatigue analysis with an objective of preventing slab cracking. All the calculations of current finite computer models [13,16,24] indicate that the most critical fatigue stress occurs at the edge of the slab, midway between transverse joints, when the outside wheels of a truck are placed at the mid-slab edge of slab (Fig. 1.1a, page 10). The conclusion has been proved by the performance of jointed PCC pavements: most fatigue cracks were found initiated at mid-slab edge of slabs in the AASHO Road Test, the Michigan Road Test and in-service pavements [16,32]. The mid-slab edge position has a higher fatigue damage than the locations near joints or any other locations when the pavements were subject to the same average lane traffic. Since the joints are at some distance from this location, transverse joint spacing and type of load transfer have very little effect on the magnitude of fatigue stresses.

The lateral distribution of wheel loads also plays an important role in the fatigue analysis. The highest stress occurs when the outside truck wheels are running at the edge of slabs. As the truck placement moves inward a few inches from the edge, the stress decreases significantly. At increasing distance inward from the edge, the frequency of load applications increases but the magnitude of edge stress decreases. Theoretically, the distribution of wheel placement across the traffic lane must be known, so that the damage ratio at the pavement edge caused by each load placement can be calculated and summed up to obtain the total damage. This procedure is too cumbersome for design purposes but was analyzed by the PCA to develop a more easily applied method . In the PCA method, fatigue at the pavement edge was computed by placing the load incrementally at distances inward from the slab edge for typical distribution of truck placement. It was found that the same fatigue damage can be obtained by considering the edge loading only and placing 6% of the total number of load repetitions at the pavement edge. If the total number of repetitions are used for the design, the edge stress must be reduced to obtain the equivalent fatigue consumption. For 6% truck encroachment, the edge stress must be multiplied by an adjusting factor of 0.894. This factor was used in preparing the equivalent stress tables (Tables 9.2a & 9.2b) [23].

Pumping and Erosion

Another important type of distress, which needs to be addressed in the design of jointed PCC pavements, is the pumping and erosion of material beneath and beside the slab. Many repetitions of heavy axle loads at slab corners and edges may cause

pumping and erosion, corner breaking, and faulting of pavement joints. In fact, most of the failures in the Maryland and AASHO road tests were the results of pumping [7, 8, 13, 16, 19].

Pumping is defined as the ejection of water and subbase material through joints, cracks, and along the edge of pavements caused by slab deflection due to heavy axle loads. The sequence of events leading to pumping erosion includes the creation of void space under the pavement caused by temperature curling of the slab and plastic deformation of the subgrade, entrance of water, ejection of muddy water, enlargement of void space, and finally the faulting and cracking of the leading slab ahead of traffic. Pumping occurs under the leading slab when the trailing slab rebounds, which creates a vacuum and sucks the fine material from underneath the leading slab, as shown in Figure 1.2. It should be emphasized that pumping occurs only when the materials under the concrete slabs are saturated with free water. Other factors that influence pumping and erosion include stiffness of concrete slab, magnitude and number of repeated loads, efficiency of load transfer at the joints, amount of deflection, water pressure under slab, and permeability or drainability of subbase. No mechanistic models currently available take all of the above factors into consideration. The only practical model used by current design methods is the one developed by the Portland Cement Association (PCA) [25].

Erosion Criterion (PCA Method)

Pumping and erosion are more directly related to pavement deflection than to flexural

stresses. The PCA method of analyzing erosion is a mechanistic-empirical method that establishes correlations between finite-element calculated results (deflection of slab and pressure under slab) and AASHO Road Test performance data. The first attempt to directly relate deflection to performance was not successful because a thinner slab has a shorter deflection basin and receives faster load punches than a thicker slab with the same deflection. A more useful correlation was obtained from the power, or the rate of work done by an axle load on a unit area of a slab. The power was expressed as:

$$P = \frac{p \; w \; C}{l \; k^{0.063} \; / \; (\text{truck speed})} = 268.7p \; w \; k^{0.27} \; / \; h = 268.7 \; p^2 / \; k^{0.73} / \; h \qquad (1.11)$$

where: P = power with which an axle load deflects the slab,

p = pressure under the slab,

C = a constant,

w = corner deflection,

h = slab thickness,

l = radius of relative stiffness, (See Eq. 1.3)

k = modulus of subgrade reaction.

The development of the erosion criterion was also correlated to the joint faulting of PCC pavement performance. The allowable number of repetitions is expressed as:

$$\log N_d = 14.524 - 6.777 \; (C_1 \times P - 9.0)^{0.103} \qquad (1.12)$$

where : N_d = allowable load repetitions for an axle load to end of design period,

P = power as defined above,

C_1 = 1.00 for normal, untreated subbase, 0.90 for stabilized subbase.

The equation for erosion damage is:

$$\text{Percent erosion damage} = 100 \Sigma n_i (C_2 / N_i) \quad (1.13)$$

where: n_i = expected number of axle-load repetition for axle-group i,

N_i = allowable number of repetition for axle-group i,

C_2 = truck encroaching coefficient, 0.06 for pavements without concrete shoulders, 0.94 for pavements with concrete shoulders. With a concrete shoulder, the corner deflection is not significantly affected by the truck placement, so a large C_2 is used. The value of 0.06 for the pavements without concrete shoulder is also conservative because it is based on a study of pavements with paved shoulders [23]. Gravel, asphalt and blotter shoulders are treated as without concrete shoulder.

The total erosion damage at the end of design period should be less than 100 percent. Because the calculation of critical corner deflection involves complicated finite element analysis, equations 1.11 through 1.13 are not used in the thickness design procedure. They are used to create the design tables and design charts. The PCA method gives erosion factors (Tables 9.3a-9.3d, page 68-69), which depend on thickness of slab, subgrade-subbase k value, with or without concrete shoulder, and doweled or aggregate-interlock joints. Design charts (9.2a and 9.2b, page 70-71) show allowable N values as N_i / C_2 to save a calculation step. [23]

Critical Deflection Location for Erosion Analysis

The most critical pavement deflections occur at the slab corner when axle loads are placed at the joint with the wheels at the corner (Fig. 1.1b on page 10). A 160 kN (36 kip) tandem axle load usually causes more deflection than a 18-kip single axle load in contrast with that the latter induces higher stresses at mid-slab edge than the former. In this situation, transverse joint spacing has no effect on the magnitude of

corner deflections but the type of load transfer mechanism and concrete shoulder have substantial effects.

1. 2. 4 Current Design Methods for Jointed PCC Pavements

AASHTO Design Guide

The "AASHTO Guide for Design of Pavement Structures" was originally developed from the results of the AASHO Road Test conducted in Illinois from 1958 to 1960. The Interim Guide was published in 1962 and revised in 1972, 1981, 1986, and 1993 [7, 8]. The nature of the design method is empirical. The governing equation for rigid pavements is given as (in English units):

$$\log(W_{18}) = Z_R \times S_o + 7.35 \log(h+1) - 0.06 + \frac{\log[(P_i-P_t) / (P_i-1.50)]}{1+[1.624\times10^7 / (h+1)^{8.46}]}$$

$$+(4.22 - 0.32P_t) \times \log\left\{\frac{MR\times C_d\times(h^{0.75} - 1.132)}{215.53\ J\ [h^{0.75} - 18.24 / (E/k)^{0.25}]}\right\} \qquad (1.14)$$

where: W_{18} = predicted number of 18-kip equivalent single axle load applications,

Z_R = standard normal deviation corresponding to selected level of reliability,

S_o = overall standard deviation for rigid pavement,

h = thickness (inches) of pavement slab,

P_i = initial serviceability,

P_t = terminal serviceability,

MR = modulus of rupture (psi) for portland cement concrete used on a

specific project,

J = load transfer coefficient used to adjust for the load transfer characteristics of a specific design,

C_d = drainage coefficient,

E = modulus of elasticity (psi) for portland cement concrete, and

k = modulus of subgrade reaction (pci).

A serious limitation of the AASHTO design method is that the equation can be applied only to the conditions that are the same or similar to the road test site. In the AASHO Road Test, the construction quality was highly controlled, but a typical highway project may contain much greater construction and material variability. The AASHTO design nomograph was developed based on a slab thickness of 10 in (254 mm) and a terminal serviceability of 2.5. A correction term was then developed to approximately account for the effects of different terminal serviceability. It was reported that there was no error in predicting W_{18} for slab thickness of 10 in (254 mm), while there was a potential error of up to 1 in (25 mm) in predicting W_{18} for extreme slab thicknesses such as 6 in (152 mm) or 14 in (356 mm) [8].

Design of Zero-Maintenance Plain Jointed Concrete Pavement

The Zero-Maintenance Design procedure for JPCP was developed in 1977 [13]. The method is for the design of heavily trafficked highway pavement which will perform relatively maintenance-free over a selected design period. The term "Zero-maintenance" refers only to structural maintenance such as patching, crack filling, slab replacement, and overlay.

The first design approach was to modify the existing AASHTO Design Guide. The revised regression equations were based on both the AASHO Road Test and 10 additional field surveys from nationwide locations. The terminal serviceability was raised to meet the zero-maintenance requirement; new equations were developed; and a climatic regional factor was introduced into the design procedure. The detailed regression equations [13] are not listed here.

The second parallel approach was to add a structural design based on fatigue analysis. Finite element programs were used to compute the critical edge stresses due to both traffic loads and temperature curling. The modulus of rupture of the concrete used in a highway project varies from point to point and this variation has a significant effect on pavement performance [13, 32]. The coefficient of variation is defined as follows:

$$CV = \text{standard deviation} / \text{mean modulus of rupture} \qquad (1.15)$$

Many transportation agencies have studied the quality control of concrete. Field data indicate that the coefficient of variation ranges from 5 to 25 percent for excellent to poor quality control, respectively. It is recommended that construction control should be adequate to limit the coefficient of variation to 15 percent or less. The design PCC modulus of rupture adjusted for concrete variability is obtained from the following expression:

$$MR_{28d} = MR_{28} (1 - C \times CV) \qquad (1.16)$$

where MR_{28} = mean modulus of rupture at 28 days,

MR_{28d} = design modulus of rupture at 28 days,

CV = coefficient of variation,

C = 1.03, a constant representing a confidence level of 85 %.

The concrete strength gain with age was also considered in the fatigue analysis. The static flexural strength at given time is given as:

$$S_c = F_A \times MR_{28d} \tag{1.17}$$

where $F_A = 1.22 + 0.17 \log T - 0.05 (\log T)^2$

T = time since the pavement slab was constructed, years,

MR_{28d} = design modulus of rupture at 28 days.

The allowable axle load applications used in the design is given as Eq. (1.8) on page 8. The final design must satisfy both the serviceability criterion and the fatigue criterion. With the additional field survey data, a new design approach, and narrowed subject (zero-maintenance JPCP only), the design procedure reaches higher reliability than the AASHTO Design Guide. It is important to keep in mind that the Zero-Maintenance Design Procedure for JPCP is for heavy truck traffic, and concrete slabs with thicknesses ranging from 203 mm (8 in) to 356 mm (14 in). Any concrete pavement slab less than 203 mm (8 in) thick should not be designed by this method. Another limitation of the method is that pumping and erosion of subbase material are not directly considered in the design.

PCA Thickness Design for Concrete Highway & Street Pavements

The well known version of the PCA thickness design procedure for concrete pavements was first published in 1966 [24]. The current revised version [23, 25] was released in 1984 with a new pavement foundation erosion criterion and the

conventional fatigue criterion for thickness design. A finite element computer program called JSLAB was employed to calculate the critical stresses and deflections, which were then used in conjunction with the design criteria to develop the design tables and charts. The design procedure is based on theoretical studies, research experience, and observations of performance of pavements including both the AASHO Road Test results and studies of pavement faulting. The fatigue and erosion criteria of the PCA method have been discussed in section 1.2.3. The other features are summarized as follows:

1. Concrete Properties - The only material property input required is the average modulus of rupture of concrete determined at 28 days using the method specified by ASTM C78 standard test. In view of the fact that variations in modulus of rupture have a significant effect on pavement performance, the modulus of rupture is reduced by one standard deviation (a coefficient of variation of 15 % is assumed). The strength gain with age is also considered but the amount of the adjustment is not known. The designer simply inputs the average 28-day flexural strength because both reduction due to variation and gain due to age has been incorporated in the design charts and tables.

2. Transverse Joints - The following values are used for the computer program input: dowel bar diameter = 1/8 of slab thickness; modulus of dowel-concrete reaction = 2,000,000 pci (543 GN/m^3); shear spring constant for aggregate interlock = 5000 lb/in/in (34.5 GN/m/m).

3. Subgrade and Subbase Support - Three types of subbase (untreated, cement-treated, and lean concrete) are suggested in the procedure. The effective modulus of

subgrade reaction k-value at the top of subbase is estimated from information of the k-value of subgrade soil, and the thickness and type of subbase. Average k-value in normal summer and fall is used without considering the variation over the year.

4. Traffic - The data on average daily truck traffic (ADTT), direction distribution factor, lane distribution factor, and axle-load distribution are used to calculate the repetitions for each group of single-axle or tandem-axle loads. The design procedure also provides several typical axle-load distributions when actual axle-load data are not available.

5. Load Safety Factor (LSF) - The axle loads are multiplied by a load safety factor to compensate for the possibility of unprotected heavy truck overloads and normal construction variations in material properties and slab thickness. For interstate and other multilane projects where there will be uninterrupted traffic and high volume of truck traffic, LSF = 1.2; for highways and arterial streets with moderate volumes of truck traffic, LSF = 1.1; and for roads and streets with low volumes of truck traffic, LSF = 1.0.

6. Temperature Curling and Moisture Warping - Curling stresses are not considered in the fatigue analysis for several reasons: a) Joints are used to relieve curling stresses The procedure recommends that the maximum joint spacing is 4.6 m (15 ft) for nondoweled plain concrete pavements, and 6.1 m (20 ft) for plain-doweled pavements. b) Curling stress may be added to or subtracted from loading stresses to obtain combined stresses. c) When the fatigue principle is used for design, it is not practical to directly combine loading and curling stresses. A pavement may be subjected to millions of load repetitions during the design period, but the number of

stress reversals due to curling is quite limited. d) Furthermore, the thermal gradient varies daily, monthly and annually. Detailed data are not available in most cases.

Other researchers believe the curling stresses should be included in the fatigue analysis and consider the issue as one of the limitations of the PCA method [16]. Another major limitation is that climate and drainage factors are not included in the design procedure. The procedure suggests that the erosion criterion be modified by local experience.

1. 2. 5 Design Methods for Pavements with Fiber Reinforced Concrete

Many pioneer projects of FRC were airport related pavements (runway, taxiway and terminal apron). Parker (1974) developed a pavement thickness design method for steel fiber reinforced concrete similar to the methods for conventional concrete. The allowable working stress of SFRC aircraft pavements was set at 80 percent of the modulus of rupture obtained from the laboratory SFRC specimens [27]. Ernest Schrader (1984) considered the improved fatigue strength and strength gain due to age into his design method for SFRC with an illustrative example of airfield pavement [31]. Pumping or erosion was not taken into account by either case simply because it is not a major distress of airport pavements. Aircraft pavements are usually much thicker than highway pavements and they are built on stabilized subbases. It is also an important fact that the loads are applied far away from the edge of airport pavements but near the edge of highway pavements, which results in different stresses, deflections, and distress models.

2. OBJECTIVES

1. To identify the most important mechanical properties of fiber reinforced concrete through discussing the test results from compressive strength tests, static elasticity tests, static flexural tests and fatigue flexural tests, and establish the equations required for fatigue analysis.

This objective is accomplished through chapters 5, 6, and 7, which discuss the test results, compare the differences between plain concrete and FRC, and explain why flexural toughness is not used as a design factor and why flexural fatigue strength is considered important.

2. To develop a thickness design method for jointed FRC highway and street pavements, adapting the current PCA design method and incorporating the distinctive fatigue properties of FRC.

This objective is accomplished through chapters 8 and 9. The PCA "Thickness Design for Highway and Street Pavements" is modified by changing the fatigue endurance limit and fatigue S-N function based on the test results of the SFRC. Because the SFRC studied has practically the same stiffness as plain concrete, the erosion design criterion, which is controlled by slab deflection and pressure under the slab, is used without change except the steel fiber reinforcement is assumed to have load transfer capacity similar to conventional dowels in the thin (less than 180 mm or 7 in.) pavements.

3. To evaluate the performance of jointed FRC pavements constructed on Haines Avenue, Rapid City, South Dakota, in 1988.

After seven-year service, the SFRC test sections on Haines Avenue was inspected on May 21, 1995, in accordance with " Distress Identification Manual for the Long-Term Pavement Performance Project" [30]. The findings are reported in chapter 10.

3. RESEARCH SIGNIFICANCE

A modified design method based on experimental investigation and field application of FRC was developed. The method provides an alternative pavement design and also reveals that the utilization of FRC is most beneficial in preventing fatigue cracking of pavements.

4. EXPERIMENTAL PROGRAM AND FIELD APPLICATIONS

Task 3: The task of this chapter is to summarize the experimental program and field applications. The following information is provided: 1) The location and geometrical dimensions of the field test sections of SFRC pavements. 2) The SFRC mix proportions and material description. 3) Test specimens made and curing conditions.

This research is the continuation of two research projects under the leadership of Professor Ramakrishnan (Dept. of Civil Engineering, South Dakota School of Mines and Technology) and sponsored by the South Dakota Department of Transportation [1, 2]. Steel fiber reinforced concrete with 0.5 percent fiber content by volume was used in the construction of pavements on Haines Avenue and Sheridan Lake Road, Rapid City, South Dakota. A large number of test specimens were made from the field concrete mixes and their basic properties were evaluated.

4.1 Field Applications

Haines Avenue from I-90 to E. North Street in Rapid City - This was a federal aid urban systems reconstruction project, 737.3 meters (2419 ft) long, 14.6 meters (48 ft)

wide roadway plus curb and gutter. It was designed with a 190 mm (7.5 in) plain concrete slab without dowels at transverse joints (The original design was based on the AASHTO design method and then modified by local experience). The steel fiber reinforced concrete pavements, which are located between intersecting Custer Street and Van Buren Street, consist of two sections: one is 27.4 m (90 ft) with 152 mm (6 in) thickness and the other is 22.9 m (75 ft) with 127 mm (5 in) thickness. There are three transition sections each of 4.6 m (15 ft) between the two sections and between plain concrete and SFRC sections. Transverse joint spacing is 4.6 m (15 ft) and longitudinal joint spacing is 3.7 m (12 ft), center to center. The concrete was supplied by a central ready mix plant. Both plain concrete and FRC pavements were conventionally placed and finished using a concrete paving machine. The project was constructed in June 1988 [2].

Sheridan Lake Road from Corral Drive to South City Limits, Rapid City - The road is 14.6 m (48 ft) wide plus curb and gutter. Plain, steel fiber (hooked end steel fiber and corrugated steel fiber) reinforced concrete and polyolefin fiber reinforced concrete pavements were cast in different sections along the road. The concrete mix design, the joint spacing, and the mixing and placing procedures were the same as in the Haines Avenue project. The SFRC with the same 0.5 % hooked end steel fibers was used at the intersection of Corral Drive and Sheridan Lake Road. The intersection was constructed with 140 mm (5.5 inch) SFRC slabs in 1994 [1].

4.2 Mix Design and Materials

Fiber reinforced concrete is a composite material. The performance of FRC pavement is a consequence of its composite materials, the mix design and the quality of the construction. The mechanism of how fibers strengthen concrete is related to the fiber properties (elastic modulus, strength, fiber end anchorage features, aspect ratio, and fiber content), concrete properties (strength, elastic modulus, and shrinkage parameters), and the properties of the interface between the fibers and concrete matrix. To achieve desirable workability of FRC and create enough cement paste to coat all aggregate and fiber surfaces, higher cement content than plain concrete was usually used in the past. However, higher cement content makes FRC more sensitive to drying shrinkage and differential temperatures, which results in curling of FRC slabs. It was reported that instead of fatigue failure, corner cracking became a major distress of FRC pavements due to curling and lost support of subbase [29, 31]. Continuing research and field practice led to the incorporation of fly ash in FRC technology. There are four advantages of replacing cement with fly ash. First, it is more economical. Fly ash is less costly than Portland cement and is readily available as a by-product of combustion of coal for power generation. Second, fly ash enhances workability of FRC mix. One of the principal ingredients of fly ash is silicon oxide that has a sphere-like molecular structure and affords the FRC a "ball-bearing" action. Third, it produces less hydration heat than cement and helps to control the curling effect of FRC pavements. Lastly, it increases long-term strength gain of FRC.

Based on the research experience of Professor Ramakrishnan, the mix proportion listed

in table 4.1 was selected to give a minimum compressive strength of 38 MPa (5500 psi).

Table 4.1 Basic Mix Proportions for The SFRC

Cement	311 kg /m^3	525 lb /cu. yd
Fly Ash	67 kg /m^3	113 lb /cu. yd.
Coarse Aggregate	969 kg /m^3	1634 lb /cu. yd
Fine Aggregate	790 kg /m^3	1331 lb /cu. yd.
Fibers	39 kg /m^3	66 lb /cu. yd.
Water/(Cement + Fly Ash) Ratio	0.39 - 0.41	
Water/Cement Ratio	0.48 - 0.50	

The fibers used were hook end steel fibers designated as ZC 60/.80, i.e. 60 mm (2.36 in) long and 0.80 mm (0.031 in) in diameter. They were bundled with water soluble glue and distributed uniformly in concrete during the normal mixing procedure. The minimum tensile strength of the fibers is 1172 MPa (170,000 psi) and the aspect ratio is 75. Two kinds of coarse aggregates were blended, which have the maximum sizes of 19 mm (3/4 in) and 38mm (1.5 in), respectively. The fine aggregate used was natural sand from Birdsall Sand & Gravel Co., Rapid City. Both the coarse and the fine aggregates satisfied grading requirements in accordance with the ASTM C33. Cement used was type I/II cement and conformed to the requirements of ASTM C150. Fly ash conformed to ASTM C618. Air entraining agent (Neutralized Vensol Resin produced by Master Builders) was used to improve concrete durability and workability.

Two trial SFRC mixes were made before the road construction and designated as SDI and SDII. The field mixes were designated as SDPI and SDPII. The control plain concrete was taken from field mix SDPI before adding steel fibers and named as SDPI-P.

4.3 Test Specimens

Test specimens were made for compressive strength, static modulus of elasticity, static flexural, and flexural fatigue tests. All specimens were cast in steel molds using a mechanical vibrator for proper compaction of the concrete. After casting was over, the specimens were covered with plastic sheets until the next day when they were demolded and placed in lime saturated water for curing. The specimens were taken out of the tanks at the specific age for testing. The beams for fatigue testing were taken out of the tanks at the age of 28 days and painted with a curing compound (Protex Promulsion).

5. COMPRESSIVE STRENGTH AND STATIC MODULUS OF ELASTICITY

Task 4: Identify the most important properties of FRC to be used for the FRC pavement design, compare the differences between plain concrete and FRC in design factors, and establish the equations for fatigue analysis of FRC pavements. Task 4 is accomplished through chapters 5, 6 and 7. The task of chapter 5 is to summarize and discuss the test results from compressive strength test and static modulus of elasticity test. Comparison between plain concrete and SFRC is also made through table and figure.

The 28-day compressive strength is an important quality control property because the concrete with higher compressive strength is more durable and has better resistance to the surface wear from studded tires. The static modulus of elasticity test for both plain concrete and SFRC justify that the elastic plate theory used for the analysis of plain concrete pavements is still valid for SFRC pavements.

The 152 $\times$ 305 mm (6 $\times$ 12 in) cylinders were tested for static modulus of elasticity (ASTM C469) and then for compressive strength (ASTM C39). The average values obtained from 28-day tests are given in Table 5.1 on page 32.

It was observed that 0.5 % fibers by volume had no significant effect on either compressive strength or static modulus of elasticity. When all the mixes had the same mix proportions and water/cement ratio, the air content (tested in the field in accordance with the ASTM C231) became the major factor of compressive strength. Figure 5.1 shows the relationship between the compressive strength and air content of concrete. For the compressive strength, the coefficient of variation within-batch varied from 3 percent to 9 percent. The average strength of the four SFRC mixes was 40.96

MPa (5940 psi), exceeding the minimum compressive strength of 38 MPa (5500 psi) required. The overall coefficient of variation for all SFRC was 10.8 %. This value presents not an excellent but a good quality control, which is close to a field situation rather than strictly controlled laboratory conditions. The average modulus of elasticity of SFRC mixes was 3.65×10^4 MPa (5.30×10^6 psi) with a coefficient of variation of 4 %. If the plain concrete was included, the overall average became 3.68×10^4 MPa (5.34×10^6 psi) with the same coefficient of variation of 4 %. The test results indicate that when the volume percentage of steel fibers is only 0.5 %, the elasticity of SFRC is practically the same as the plain concrete. The previous research also reported that the effect of steel fibers on elasticity of concrete is negligible if fiber content is less than 2 percent [2-6, 10]. This conclusion means that the stiffness of SFRC is the same as plain concrete and all structural analysis methods based on small deformation theory of an elastic medium-thick plate are valid for both plain concrete and SFRC pavements.

Table 5.1 - Compressive Strength, Static Modulus and Air Content

Mix Type, and Mix Number	Compressive Strength MPa (psi)	CV * (%)	Static Modulus 10^4 MPa (10^6 psi)	CV * (%)	Air Content (%)
SFRC, SDI	45.9 (6650)	5	3.72 (5.40)	2	3.6
SFRC, SDII	35.5 (5150)	3	3.45 (5.00)	2	6.9
SFRC, SDPI	40.0 (5800)	4	3.72 (5.40)	2	5.8
SFRC, SDPII	42.5 (6170)	9	3.66 (5.31)	0.4	4.3
Plain, SDPI-P	39.6 (5740)	4	3.86 (5.60)	1	5.8

* CV = Coefficient of Variation

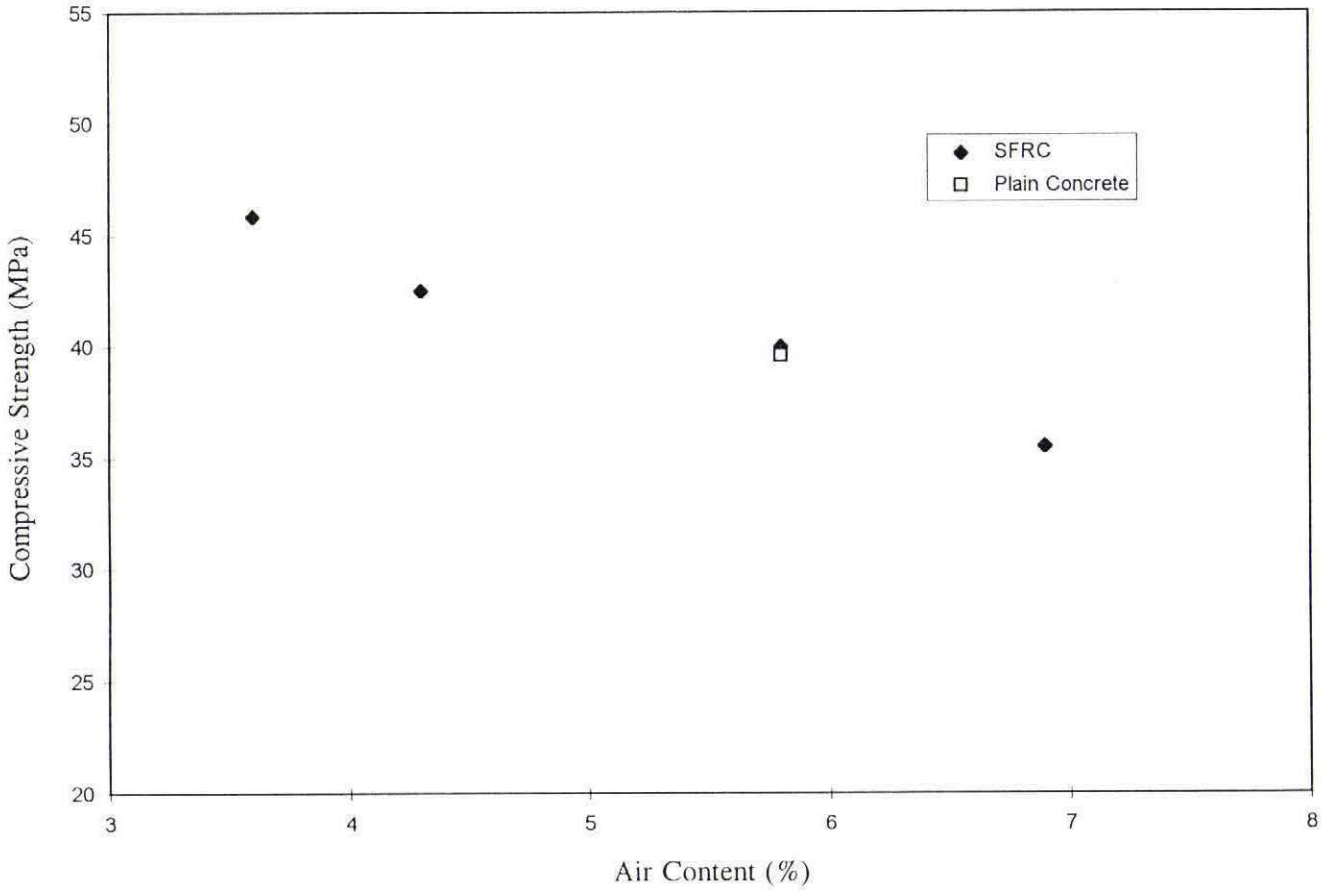

Fig. 5.1 Effect of Air Content on Compressive Strength

6. FLEXURAL TESTS UNDER STATIC LOADING

Task 4 (Continued): The task of this chapter is to discuss the test results from flexural test under static loading and identify the important material properties for FRC pavement design. Explanation is given why flexural toughness is not used as a design factor and why flexural strength, its variation and its growth with age are important for FRC pavement thickness design.

When plain concrete is used, flexural strength, termed as modulus of rupture, is often the only concrete material property input for pavement thickness design. Plain concrete is a brittle material that fails simultaneously with the appearance of a crack. The main difference in behavior between SFRC and plain concrete under static loading is SFRC's ability to support loads even after the formation of cracks. The fiber reinforcing effect varies from substantial to subtle depending upon a large number of variables. The fibers with high modulus of elasticity and high degree of surface bonding and end anchorage generally perform better.

Load-Deflection Curve - The different load-deflection curves are shown in Fig. 6.1. For many practical applications with fiber content about 1.5 % or less by volume, the matrix first-crack strength is not changed much by the introduction of fibers. The first crack occurs at the point on the load-deflection curve at which the form of the curve first departs the elastic linear behavior. Under static loading, a FRC beam fails in one of the three models following first cracking (Fig. 6.1):

Model 1. - The FRC composite continues to carry increasing loads after matrix cracking. The peak load-carrying capacity and the corresponding deformation are greater than those of plain concrete. During the inelastic range of this ductile failure

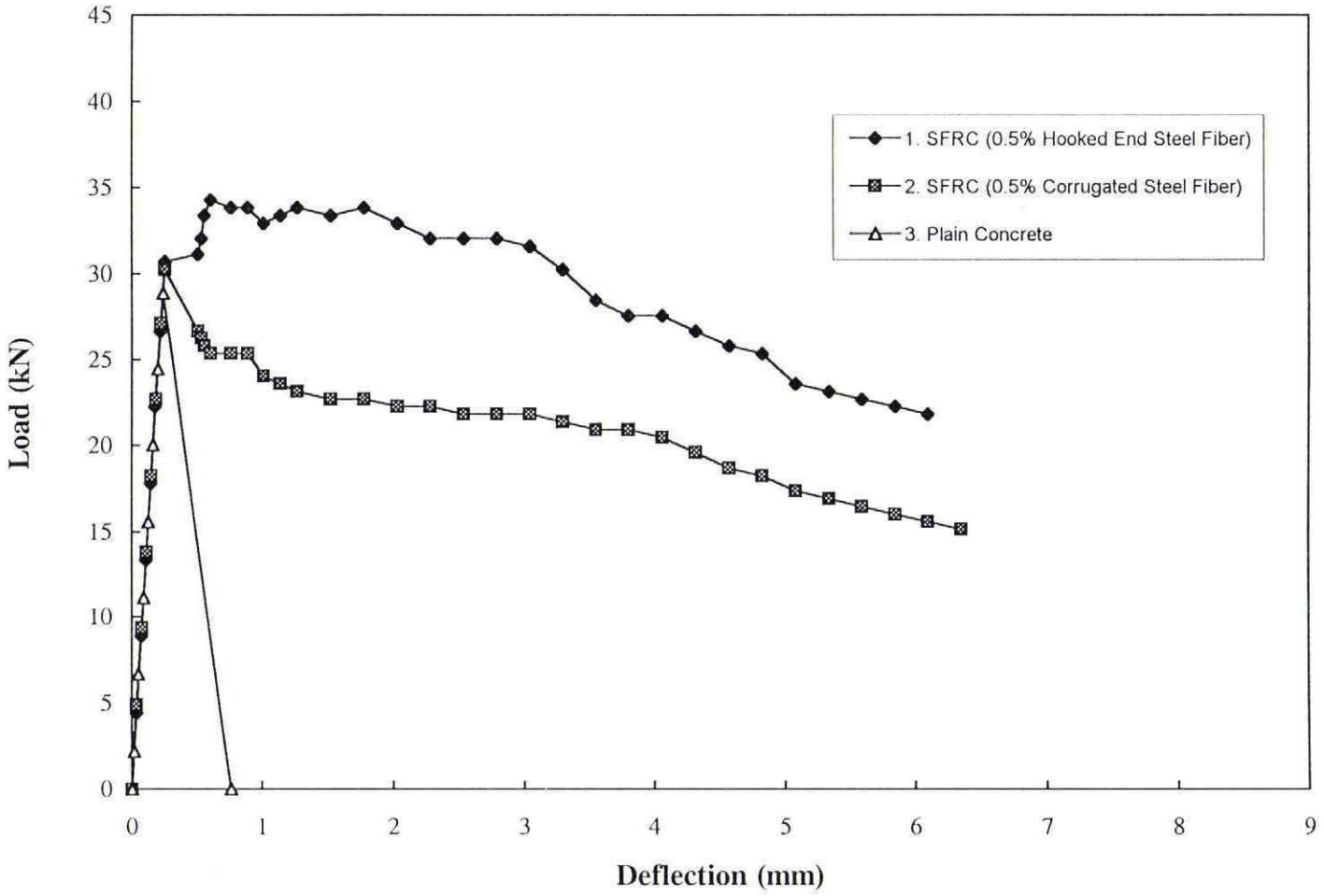

Fig. 6.1 Typical Load-Deflection Curve

model, progressive debonding, frictional slippage at fiber-matrix interface, and some additional matrix cracking occur. If the fibers used have sufficient bond strength and end anchorage, fiber fracture also occurs, which indicates the high level of fiber efficiency. Curve 1 shown in Fig. 6.1 is an actual test curve of beam No. SDP1-A1 (hooked end steel FRC).

Model 2. - The FRC composite continues to carry decreasing loads after matrix cracking. The drop occurs either at the first crack or right after it. The post-cracking resistance is primarily attributed to fiber pull-out. While considerable enhancement of fracture energy is obtained, no significant increase in flexural strength is observed. Curve 2 shown in Fig. 6.1 is an actual test curve of beam SDSP-B5 with 0.5 % corrugated steel fibers. SFRC with 0.5 % -1.0% straight steel fiber content has similar load-deflection curve [3, 6, 10].

Model 3. - Similar to plain concrete, shown in Fig. 6.1, the FRC composite may fracture immediately after first cracking. This type of brittle failure results from inadequate fiber content at the critical section. It was reported that FRC with 0.1 % polypropylene fibers often failed this way [21].

It was observed that if the concrete mix design was the same, the stiffness of plain concrete and FRC is about the same under static flexural loading until the first crack point. This conclusion was also confirmed by previous literature [3-6, 10, 21]. The region from the origin to the first crack point is called the elastic region in which the performance of both plain concrete and FRC practically depend on concrete matrix only and the load-deflection relationship is linear. For design of concrete pavement,

the traffic loads are not allowed to exceed the first crack point regardless of whether concrete is plain or fiber reinforced. It is obvious that plain concrete and FRC without adequate fibers at the critical section fail immediately with the first cracking. For FRC with model 1 or model 2 failure under static loading, traffic loads are not allowed to be greater than first crack load either. The reason is that traffic loads are not static but repetitive fatigue loading. Both magnitude of loads and number of repetitions must be taken into account in pavement design. If the magnitude of a load is great enough to cause the first crack at the first cycle of loading, the number of repetitions to failure will be very low, typically less than 100. Concrete reinforced by discontinuous,random distributed fibers with fiber content ranging from 0.5 % to 1.5 % by volume cannot allow cracks in the same way as continuous reinforced concrete pavements (CRCP), which was a lesson learned from early applications of FRC [29]. Because all traffic loads are limited below the first crack load, the analysis of stresses and deflections for plain concrete based on elastic medium-thick plate theory should also be valid for FRC.

Toughness - Toughness is generally accepted as a measure of energy absorption capacity of a material. Nevertheless, the debate on how it should be measured, interpreted, and used in design is still inconclusive [38]. In many cases the toughness properties tested by different methods are not only material dependent but also influenced by many testing factors such as specimen size (depth, width, span), loading configuration (mid point or third point loading), load rate and control, accuracy of measurement of first crack deflection, test machine stiffness, and so on. A great deal

of research interest has been shown in the development of a test standard to evaluate toughness performance. A static third-point bending configuration is used in the "Standard Test Method for Flexural Toughness and First-Crack Strength of Fiber-Reinforced Concrete" (ASTM C1018). The preparation of the specimen and the loading system are the same as in the "Standard Test Method for Flexural Strength of Concrete" (ASTM C78). The toughness or the energy absorbed by the specimen is computed from the area under the load-deflection curve. To minimize the effects of specimen size and the other testing factors, the energy absorbed by a specimen up to a certain deflection level can be normalized by dividing it by the energy absorbed up to first crack, which produces a dimensionless parameter called toughness index. According to ASTM C1018, the toughness indexes I_5, I_{10}, and I_{20} are calculated ratios of the area of the load-deflection curve up to the deflections of 3, 5.5, an 10.5 times the first-crack deflection divided by the area under the same load-deflection curve up to the first crack, respectively. Toughness indexes are not used in this thickness design for several reasons:

1. The toughness indexes are based on the value of the first-crack deflection that is very small and too sensitive to testing errors. Any extraneous deformations may introduce significant error up to more than 100 %, making the test value of first-crack deflection useless. The specimens made from the same mix but tested in different laboratories yielded different results especially in the values of first-crack deflections [38].

2. Toughness indexes were observed to be relatively insensitive to fiber type, and fiber content [10, 38].

3. The toughness test is conducted under static loading. The major portion of the energy is absorbed by FRC after the first cracking. Because cracks are not allowed under the first cycle of loading as mentioned before, toughness indexes calculated by ASTM C1018 do not present the failure style of rigid pavements under traffic loads.

First-Crack Strength and Modulus of Rupture - The beams were tested for first-crack strength and modulus of rupture at 28 days in accordance with the ASTM C1018 and the ASTM C78. Both 365×102×102 mm (14×4×4 in) and 533×152×152 (21×6×6 in) beams were tested. First-crack strength is defined as the stress corresponding to the load at first crack which occurs when the load-deflection curve first becomes nonlinear. Modulus of rupture is the ultimate flexural stress based on the maximum load. The 28-day test results of flexural strength for the Haines Avenue project are summarized in Table 6.1. The values shown are the average for each mix. The grand average of modulus of rupture for the SFRC is 5.34 MPa (775 psi) with a coefficient of variation of 9.1 % between the average values of four mixes. The average ultimate strength is only slightly greater (3.3 %) than the that of plain concrete (5.17 MPa or 750 psi). Compared to the coefficient of variation, this increase is not significant.

The average modulus of rupture of the SFRC in the Haines Avenue project is 5.4 % greater than the average first-crack strength. Although the ultimate strength of the SFRC is only slightly greater than the first-crack strength, it characterizes a ductile failure like model 1 shown in Figure 6.1. Because it is easer and more accurate to determine the modulus of rupture (measurement of deflection of test beam not involved) and the increase of the ultimate strength is a good indicator of fiber-reinforcing effect, the 28-day

modulus of rupture is chosen as the basic design factor with the consideration of variation of concrete strength and strength gain with age.

Table 6.1 First-Crack Strength and Modulus of Rupture

Mix Type, and Mix Number	First-Crack Strength		Modulus of Rupture	
	MPa	psi	MPa	psi
SFRC, SDI	5.08	737	5.14	745
SFRC, SDII	4.29	622	4.83	700
SFRC, SDPI	5.67	822	5.96	865
SFRC, SDPII	5.22	758	5.45	790
Average of SFRC Mixes	5.19	735	5.34	775
Plain, SDPI-P	5.17	750	5.17	750

Variation in Modulus of Rupture - Variations in flexural strength of SFRC have greater effect on thickness design than variations in other material factors such as modulus of elasticity and modulus of subgrade reaction. Under normal construction practice, concrete strength has a coefficient of variation of 10 % to 12 % for good quality control, which can go up to 20 % or more for poor quality control. In the PCA thickness design [25], a coefficient of variation of 15 % is assumed, which presents fair-to-good quality control. The same value is used for this FRC pavement design. The variations in concrete strength are taken into account by selecting a design modulus of rupture 15 % lower than the mean. The design flexural strength at 28 days can be expressed by the equation:

$$MR_{28d} = MR_{28} (1- CV) = MR_{28} (1- 0.15) = 0.85\ MR_{28} \qquad (6\text{-}1)$$

where MR_{28} is the mean modulus of rupture at 28 days determined by ASTM C78, and CV is the coefficient of variation. It should be noticed that the specimens for the ASTM C78 test are usually made from one or a few batches, which may produce lower variation of test results. The coefficient of variation of 15 % assumed here is for concrete throughout a pavement project.

Concrete Strength Gain with Age - It is well accepted that concrete strength continuously increases with age because of continued hydration. Both the PCA Thickness Design [25] and the Design of Zero-Maintenance Plain Jointed Concrete Pavement [13] consider the strength gain with age. After analyzing the data from the PCA and additional data from five projects in different states, Darter proposed a regression equation for the strength gain of plain concrete as follows [13]:

$$F_A = 1.22 + 0.17 \log T - 0.05 (\log T)^2 \qquad (6.2)$$

where F_A = ratio of the modulus of rupture at time T to the modulus of rupture at 28 days,

T = time since slab construction in years.

Previous research on FRC has reported that FRC gains more strength with age than similar concrete without fibers [1-6, 14]. For the FRC used in this research, the average modulus of rupture tested at different ages are shown in Table 6.2 and Figure 6.2. The average flexural strength at 60 days was 7.38 MPa (1070 psi), which was 38 % greater than the 28-day strength of 5.34 MPa (775 psi). The presence of fly ash apparently contributed to this substantial increase. In addition to gaining strength

through the concrete matrix in the same way as plain concrete, FRC may gain extra flexural strength through the increase of bonding strength between concrete and fibers. The average 60-day strength can be used to estimate the major strength gain with age.

$$F_A = MR_{60} / MR_{28} \qquad (6.3)$$

This approach is conservative because the 60-day strength is used for the entire design period (usually 20 years). It should be realized that the rate of strength gain depends on type of cement, use of fly ash, mix design of concrete, and other factors. Adding different types of fibers with different fiber content makes it even more difficult to predict the flexural strength gain factor. For any specific FRC, the estimate of the strength gain factor should be based upon the test data of the FRC.

The design flexural strength used in fatigue analysis can be obtained from the combination of Equations 6.1 and 6.3.

$$S_c = F_A (MR_{28})(1- CV) \qquad (6.4)$$

Table 6.2 Change in Modulus of Rupture with Age

Age of Concrete (day)		28	36	43	60
Average Modulus of Rupture	MPa	5.34	5.62	6.96	7.38
	psi	775	815	1010	1070

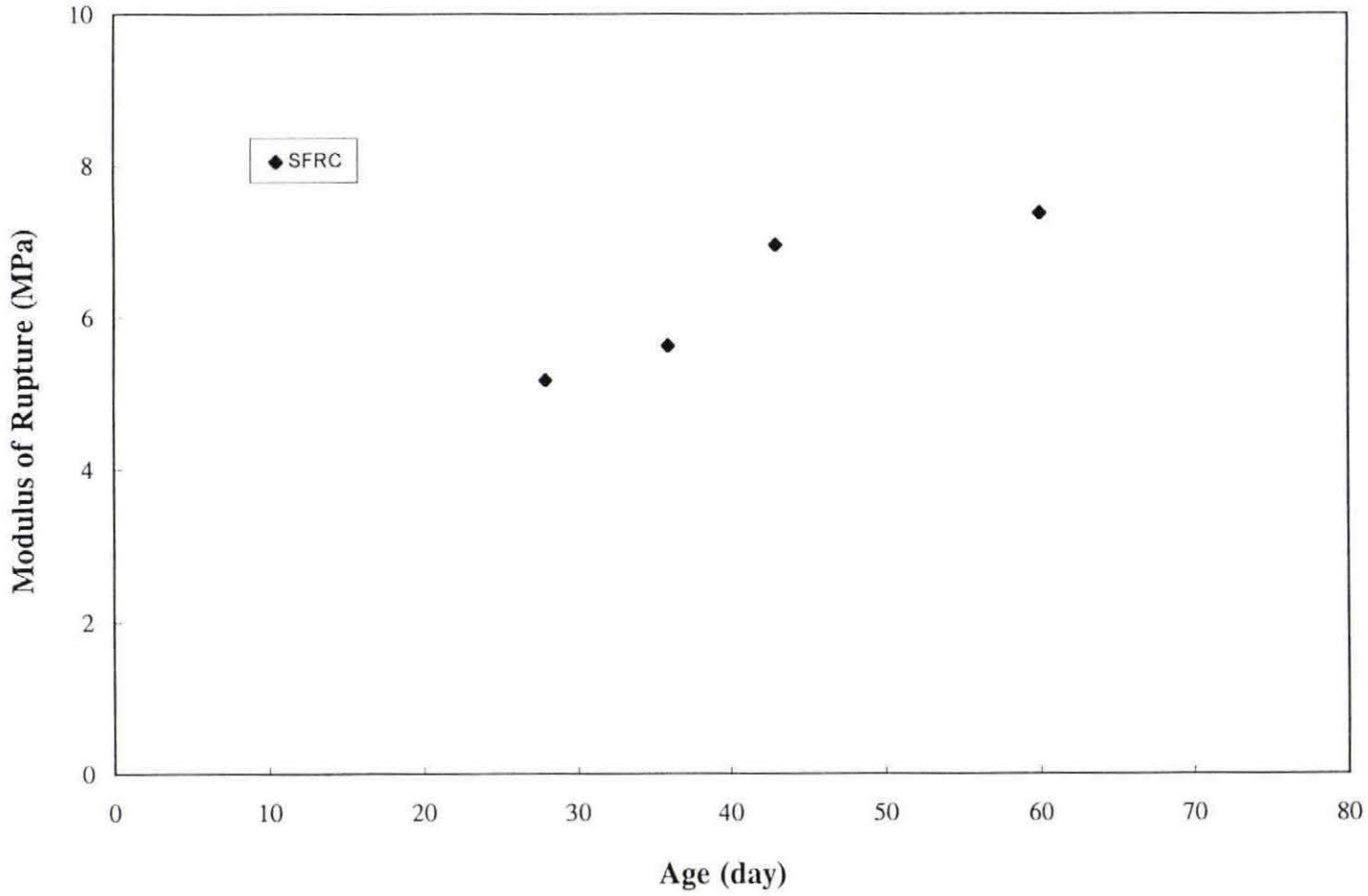

Fig. 6.2 Change in Modulus of Rupture with Age

7. FLEXURAL TESTS UNDER FATIGUE LOADING

Task 4 (Continued): The task of this chapter is to discuss the test results from flexural test under fatigue loading, identify the unique fatigue property of the SFRC used in this project, and establish the equations for fatigue design criterion of the SFRC pavements. The equations are derived from the fatigue test data and statistical analysis.

One of the greatest benefits to be gained by adding fiber reinforcement in PCC pavements is the increased fatigue strength, which prevents slabs from cracking under repetitive traffic loads. Similar to flexural strength under static loading, the performance of FRC under fatigue loading varies substantially depending on numerous factors. The fatigue properties of steel FRC are different from those of synthetic FRC. Even within the SFRC category, fiber aspect ratio, fiber content, fiber end anchorage mechanism, fiber-concrete bond strength and mix design of SFRC have significant influence on the performance of the final composite products. For any specific FRC, the design factors such as endurance limit and fatigue S-N relationship have to be determined by material tests.

In this investigation, after the 28-day static flexural tests, the remaining beams were tested under fatigue loading at ages between 36 to 60 days. The test configuration was the same as the static flexural test (ASTM C78) with third point loading. At beginning of the test, three beams from each group (same mix, same size) were tested under static loading to obtain the modulus of rupture at the same age as the reference of fatigue stress ratio for the rest beams in the group. An MTS testing machine was used for both static and fatigue tests. Non-reversing fatigue loading was applied by an electrohydraulic system operating in a load-control mode. The loading cycles had a

sine-wave shape and a frequency of 20 cycles per second. The lower limit for the dynamic loading was set at 10 % of the average maximum load from the static flexural test to prevent horizontal movements of the beams during testing. The upper limit varied from 60 % to 95 % to find the fatigue endurance limit (stress ratio with no failure after two-million-cycle loading) and S-N relationship. Fatigue test data were collected from both Haines Avenue and Sheridan Lake Road projects. A total of 62 beams from different mixes, but the same composition of SFRC, were tested.

The fatigue test results are listed in Table 7.1 and plotted in Figure 7.1. The plot shows a large scatter of data, which is typical for fatigue test results. It is observed that the percentage of survival increases as the stress ratio decreases. At a stress ratio of 95%, only 1 beam (17 % of 6 beams) survived two-million-cycle loading, while at a stress ratio of 70 %, 8 beams (75 % of 12 beams) survived. When the fatigue stress ratio was below 65 %, no failures occurred up to two-million-cycle loading. A least square regression curve (mean curve) was fit to the data as shown in Figure 7.1, and expressed as :

$$\log N = 44.65 - 48.73 \, (\sigma / S_c) \qquad (7.1)$$

where N = number of load applications,

(σ / S_c) = fatigue stress ratio,

σ = upper limit of fatigue stress,

S_c = static flexural strength.

Because no failure occurred at the stress ratio equal to or less than 65 %, the test data at a stress ratio of 65 % and below were neither included in the regression process

Table 7.1 Fatigue Stress Ratio (σ/S_c) and Number of Cycles to Failure (N)

σ/S_c (%)	N	σ/S_c (%)	N	σ/S_c (%)	N	σ/S_c (%)	N
95	100	85	50	75	600	65	2000000
	400		100		1200		
	1800		1000		1214100		
	2200		113800		2000000		
	1207500		118500		2000000		
	2000000		802600		2308600		
			1151900		2327800		
			2000000		2352400		
			2000000		2309500		
90	700	80	200	70	2200	60	2000000
	1000		2100		70200		2000000
	2500		4700		655700		2000000
	74400		842900		2000000		2000000
	84100		2000000		2000000		2000000
	49500		2000000		2000000		2000000
	2000000		2000000		2000000		
	2000000		2000000		2000000		
			2000000		2000000		
			2000000		2000000		
			2000000		2000000		
			2024300				

Note: The beams subjected two-million-cycle loading or more did not fail.

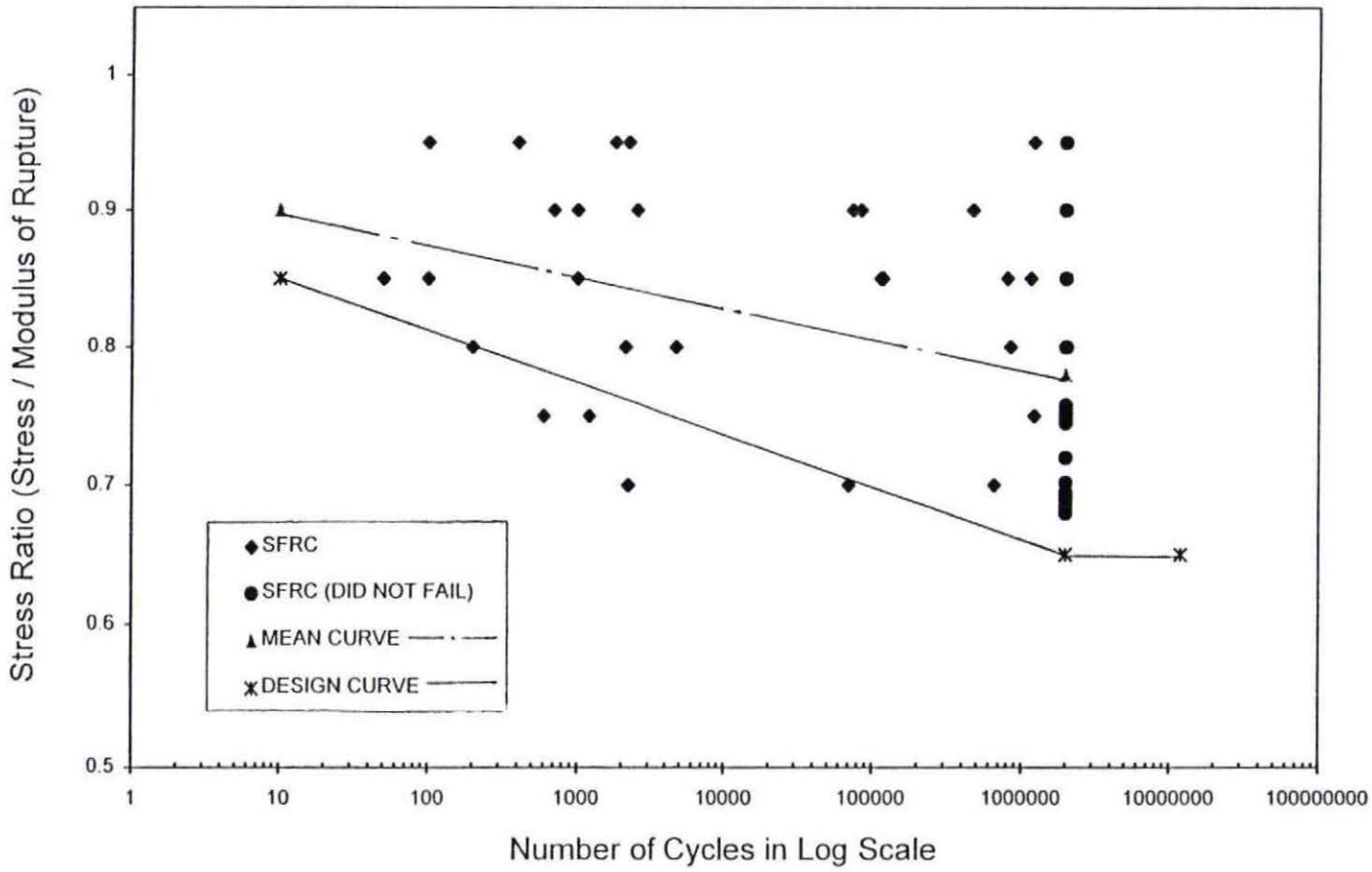

Fig. 7-1 Fatigue Stress Ratio vs. Number of Cycles (S-N Curve)

nor plotted in Figure 7.1. Some beams sustained more than two-million cycles, but they were treated the same as the beams that were stopped from the fatigue test after two million cycles. Equation 7.1 is a mean regression curve that represents a failure probability of 50 percent. According to this mean S-N curve, the fatigue stress ratio corresponding to two million cycles is 78.7 %. In other words, at the stress level of 78.7 % of the static flexural strength, probably 50 % of the beams may fail before the two-million-cycle loading and 50 % may survive. For design purposes, the mean curve has to be lowered to increase the reliability. To obtain the similar degree of conservatism for the SFRC as the PCA method for conventional concrete, a design curve (Fig. 7.1) was selected by dividing the left side of equation 7.1 by two:

$$\log N_d = 22.33 - 24.37\ (\sigma / S_c), \qquad \text{for } (\sigma / S_c) \geq 0.658 \tag{7.2}$$

This expression represents a failure probability of 3.4 percent. The design endurance limit at two million cycles is 65.8 %. If the stress level is bellow 65.8 %, the number of repetitions of loading is considered unlimited:

$$N_d = \text{unlimited}, \qquad \text{for } (\sigma / S_c) \leq 0.658 \tag{7.3}$$

It should be mentioned that equations 7.1 through 7.3 are valid only within the data base from which it was derived. In this case, they are for the SFRC with 0.5 % hooked end steel fibers and the mix design shown in table 4.1. Only the SFRC with the same fiber type, fiber content, and similar mix design can be designed using these equations.

8. PCA EROSION CRITERION FOR FRC PAVEMENTS

Task 5: Adapt the PCA design method by incorporating the special FRC properties, summarize the design procedure, and give design examples to illustrate the design method in detail. Task 5 is accomplished through chapters 8 and 9. The task of chapter 8 is to adapt the PCA erosion criterion for FRC pavement design. The steel fiber reinforcement is assumed to have the load transfer capacity similar to conventional dowels in thin slabs (less than 180 mm or 7 in.).

In the 1984 edition of the PCA Thickness Design method [23, 25], an erosion criterion was established by correlating the pavement performance with critical corner deflections and pressure under concrete slabs. Because FRC has practically the same stiffness as plain concrete, the calculation and the erosion analysis of the PCA method should also be valid for FRC. The PCA method gives erosion factors (see Tables 9.3a-9.3d, page 68-69) that depend on slab thickness, subgrade-subbase k value, with or without concrete shoulder, and doweled or aggregate interlock joints. Gravel, asphalt and blotter shoulders are treated as without concrete shoulder. If full-depth concrete shoulders are used, either tied to concrete pavement or with only keyway and sawed joint, the concrete pavement is considered having concrete shoulders in the thickness design. However, it is recommended to use tie bars in practice.

In this investigation, contraction joints were formed by saw cutting the concrete after placement. No dowels were used for either plain concrete or SFRC slabs because the truck traffic volume is low and the slab thickness is less than 8 inches. For plain concrete slabs, the load transfer depends solely on aggregate interlock. Aggregate size and joint opening are critical to the load transfer. It is reported that large aggregates (greater than 25 mm or 1 in) have better interlock than small aggregates

(13 mm or 0.5 in) [19]. For the SFRC used, the 60 mm (2.4 in) long steel fibers surely have advantage over normal size aggregates. They act like thousands of small dowels across the contraction joints. The fiber reinforcement may enhance load transfer in two ways. First, the steel fibers across joints have their own moment and shear resistance. Second, the steel fibers form a kind of bridge over the joints, holding the adjacent slabs together and making aggregate interlock more effective than without fibers. The steel fiber reinforcement (0.5 % by volume) is assumed to have the load transfer capacity similar to conventional dowels in the thin slabs (180 mm or 7 inches in depth). The assumption is restricted to thin slabs because dowels in thin slabs do not perform very well and the enhancement due to fibers will not be overestimated. It is well known that excessive bearing stresses can develop in the concrete immediately around the dowels and cause the pavements to crack and deteriorate if concrete slabs are thinner than 180 mm (7 in.). The PCA method assumes dowel size as 1/8 of slab thickness. It also recognizes that the dowels in thin slabs are not as effective as those in thick slabs. The erosion factor for 14-inch slab with concrete shoulders and aggregate-interlock joints (k = 100, single axle, table 9.3b, page 68) is 2.04. The factor is reduced to 1.76 (table 9.3a, page 68) when dowels are used, which presents a 14 % decrease. The erosion factors for 4-inch slab without dowels and with dowels (k=100, single axle, with concrete shoulder) are 3.42 and 3.24, respectively (page 68). The decrease is only 5 %.

To accurately address the effect of fibers on load transfer over joints, further research is needed.

9. DESIGN PROCEDURE

Task 5 (Continued): The task of this chapter is to modify the PCA design method by using the unique fatigue property of the FRC and summarize the design procedure for FRC pavement thickness design. Design examples are given to illustrate the method in detail, and comparison is made between FRC and plain concrete pavement design.

The PCA "Thickness Design for Concrete Highway and Street Pavements" [15] is adapted by incorporating the unique fatigue properties of FRC. The general steps to determine pavement thickness are summarized as follows:

1. Collect traffic data in the design period.
2. Select type of joint and shoulder.
3. Determine the subgrade-subbase support (k value).
4. Determine the FRC properties (MR_{28}, F_A, fatigue S-N curve, and endurance limit).
5. Select a trial slab thickness.
6. Perform fatigue analysis.
7. Perform erosion analysis.
8. Check both accumulated fatigue and erosion damage ratios. If any one of them does not satisfy design criterion or both leave too much reserve capacity, return to step 5 or justify other design factors.

The major differences between plain concrete pavement design and FRC pavement design are in steps 4 and 6. For plain concrete pavement design, an engineer normally specifies certain compressive and flexural strengths and the contractor is expected to furnish a concrete design mix which must meet these specifications. The

average modulus of rupture at 28 days (MR_{28}) is the only material property input for the original PCA design method. Other material properties such as strength gain factor, S-N curve, and endurance limit are assumed to be the same regardless of the concrete mix design. For FRC pavement design, the procedure is somewhat reversed. The properties of FRC vary substantially. They cannot be assumed before the specific fiber type, fiber content, and mix design of FRC are realized. Although the elasticity of FRC with low fiber content remains practically the same as plain concrete, the other properties especially the fatigue S-N curve and endurance limit have to be determined before the thickness design of FRC pavements. The study presented here illustrates an example of how these properties are determined. If the same FRC mix design is to be used in the future, the equations established here are valid for the thickness design. If different FRC is to be used, strength gain factor, fatigue S-N curve and endurance limit must be determined by analyzing test data of the FRC.

The fatigue analysis is based on stresses under traffic loads and FRC fatigue properties. The nomograph provided by the PCA method cannot be used because of the change in S-N curve and endurance limit, but the slab stress analysis results can be used because the elasticity of FRC is about the same as plain concrete. The equivalent stresses shown in Table 9.2a and 9.2b on page 67 are the edge stresses multiplied by a truck encroachment factor of 0.894 [23, 25]. Theses stresses are caused by an 18 kip (80 kN) single axle load or a 36 kip (160 kN) tandem axle load. Tire sizes and dual wheel spacing are usually greater for larger trucks and heavier

axle loads. Stresses do not vary proportionally to axle loads. For traffic loads different from the 18 kip (80 kN) single axle and the 36 kip (160 kN) tandem axle, the PCA method [23] suggested that the stresses are proportional to the exponent 0.94. For example, Table 9.2b (for slabs with concrete shoulders) gives an equivalent stress of 327 psi (2.25 MPa) based on a slab thickness of 6 in (152 mm) and k value of 100 pci (27.1 MPa/m) under an 18 kip (80 kN) single axle load. For a 28 kip (125 kN) single axle loads, the equivalent stress is $(28/18)^{0.94} \times 327 = 495$ psi (3.41 MPa). The allowable number of load applications for each group of axle loads is calculated according to the new S-N curve and endurance limit.

The erosion analysis remains the same as the PCA method except that the effect of fiber reinforcement on load transfer across joints is estimated to be the same as doweled joints.

Design example (English units in calculations and design tables)

The SFRC pavements in the Haines Avenue project are analyzed to illustrate the steps in the design procedure.

1. Traffic Data (Information from Data Inventory Program, SD DOT)

Four-lane urban arterial street

Design period = 20 years

Average daily traffic in 1988, $ADT_0 = 9176$ (all vehicles in both directions)

Traffic growth projection factor, G = 1.85

Directional distribution factor, D = 0.55

Table 9.1 Axle-load Distribution Data*

1	2	3	4
Axle load (kips)	Axles per 1000 trucks including pickups	Axles per 1000 trucks excluding pickups	Axles in design period
Single axles			
26 - 28	0.91	1.50	2040
24 - 26	1.81	2.99	4080
22 - 24	2.27	3.75	5110
20 - 22	3.63	6.00	8180
18 - 20	4.99	8.25	11240
16 -18	5.44	8.99	12250
14 - 16	17.70	29.27	39900
12 - 14	19.96	33.00	44980
9 - 12	70.78	117.03	159500
6 - 9	146.55	242.31	330300
Tandem axles			
50 -52	0.45	0.74	1010
46 - 50	0.00	0.00	0
44 - 46	2.72	4.50	6130
42 - 44	4.08	6.75	9200
40 - 42	5.90	9.76	13300
38 - 40	3.18	5.26	7170
36 - 38	6.35	10.50	14310
34 - 36	6.35	10.50	14310
32 - 34	8.17	13.51	18410
30 - 32	7.26	12.00	16360
28 - 30	9.53	15.76	21480
22 - 28	24.05	39.77	54200
16- 22	44.92	74.27	101200
10 - 16	80.31	132.78	181000

* The numbers in column 2 are from a study conducted by the Data Inventory Program, SD DOT. The total number of all trucks counted is 8639 including 3414 two-axle, four-tire trucks.

Lane distribution factor, L = 0.80

Truck traffic ADTT = 2.5 % of ADT (excluding two-axle, four-tire trucks)

Axle-load distribution of all truck traffic is given in Table 9.1 columns 1 and 2 (page 56).

Traffic Calculations:

Design ADT = G (ADT_0) = 1.85 × 9176 = 16976 (The design ADT is the predicted ADT at the middle of the design life.)

Design ADTT = 0.025 × 16976 = 424.4

Daily truck traffic on the most critical driving lane = (D)(L)(Design ADTT)

= 0.55 × 0.80 × 424.4 = 186.7

Total number of trucks in the 20-year design period is:

186.7 × 365 × 20 = 1,363,000 (trucks)

To calculate the total axle-load repetitions for each group of loads, the axles per 1000 trucks in Table 9.1, column 2 should be adjusted because it includes 39.52 % (3414/8639 = 0.3952) two-axle four-tire trucks. The adjusted axles per 1000 trucks listed in Table 9.1, column 3 is obtained by dividing the data in column 2 by (1-0.3952). Column 4 is the total axle-load repetition for each load group and is calculated by the following formula:

Column 4 = Column 3 × (Total number of trucks in design period / 1000)

In this example, column 4 equals column 3 times 1363.

2. Type of Joint and Shoulder

Joints are saw cut without dowels but steel fibers are assumed to enhance load transfer over the joints. Tied concrete curb and gutter are used.

3. Subbase-Subgrade Support (k value)

The subgrade soils are heavy clay. Subbase is 3 in (76 mm) untreated gravel. The effective subbase-subgrade k value is estimated as 134 pci (36.4 MPa/m).

4. FRC Properties

MR_{28} = 775 psi (5.34 MPa)

MR_{60} = 1070 psi (7.38 MPa)

Equation 6.3 is used to calculate strength gain factor:

$F_A = MR_{60} / MR_{28} = 1070 / 775 = 1.38$

Equation 6.4 is used to calculate the static flexural strength, considering both the variation in concrete strength (CV =15 %) and the strength gain with age:

$$S_c = F_A (MR_{28})(1- CV) = 1.38 \times 775 \times (1-0.15) = 909 \text{ psi } (6.27 \text{ MPa})$$

The fatigue properties of the SFRC used are governed by equations 7.2 and 7.3 on page 49.

5. Slab Thickness

h = 6 in (152 mm)

6. Fatigue Analysis

Figure 9.1a on page 62 is a worksheet for fatigue and erosion analysis. The data in columns 1 and 3 are copied from columns 1 and 4 of Table 9.1 (page 56), respectively. To be on the conservative side, the upper limit of the load in the range is used to represent the range. The axle loads in column 1 are multiplied by a load safety factor of 1.1 for arterial streets (PCA recommendation [25]) and the results are listed in column 2. The equivalent stresses (items 10 & 12) are obtained from Table 9.2b (page 67) based on a slab thickness of 6 in (152 mm) and k value of 134 pci (36.4 MPa). The

edge stresses in column 4 are calculated by the following equations:

$$\text{Edge stress} = (\text{Equivalent stress})(\text{Factored axle load} / 18)^{0.94} \quad \text{for single axles,}$$

$$\text{Edge stress} = (\text{Equivalent stress})(\text{Factored axle load} / 36)^{0.94} \quad \text{for tandem axles.}$$

The stress ratios in column 5 are the ratios of the edge stresses over the static flexural strength (S_c). The allowable repetitions (column 6) in fatigue analysis are obtained from Equations 7.2 and 7.3:

$$\log N_d = 22.33 - 24.37\,(\sigma / S_c), \qquad \text{for } (\sigma / S_c) \geq 0.658$$

$$N_d = \text{unlimited}, \qquad \text{for } (\sigma / S_c) \leq 0.658$$

The fatigue percentages (column 7) are obtained by dividing column 3 with column 6 and multiplying by 100. The sum of fatigue percentages over all single-axle and tandem-axle loads is entered at the bottom of column 7.

7.Erosion Analysis

The erosion factors in items 11 and 13 are obtained from Table 9.3a on page 68. The steel fiber reinforcement is estimated to have the same load transfer capacity as conventional dowels. The allowable repetitions listed in column 8 (page 62) in erosion analysis are obtained from Figure 9.2a (Page 70) based on an erosion factor of 2.73 for single axles and 2.78 for tandem axles. The erosion damage percentages (column 9, page 62) are obtained by dividing column 3 with column 8 and multiplying by 100. The sum of erosion percentages over all single-axle and tandem-axle loads is entered at the bottom of column 9 (page 62).

8. Check Both Accumulated Fatigue and Erosion Damage Ratios

The fatigue analysis shows that none of the fatigue ratio exceeds the endurance limit of 65.8 percent, and the total fatigue damage is zero. The erosion analysis shows that the total erosion damage is 29.5 percent. Because both are less than 100 percent, the use of a 6 in (152 mm) slab is quite adequate. Separate calculations (Fig. 9.1b on page 63) shows that a slab of 5 in (127 mm) is not adequate since the erosion damage is 133.6 percent. If calculated backward, the 5 in (140 mm) SFRC pavements are predicted having a service life of 15 years. (The pavements have been in service for 7 years since 1988. Some minor distresses appear in the 5 in (127 mm) SFRC section, which will be discussed in the next chapter.) The third trial with slab thickness of 5.5 in (140 mm) yields the fatigue damage of zero and erosion damage of 62.8 percent (Fig. 9.1 C on page 64), which is an adequate design, too.

The fatigue analysis indicates that the SFRC used in the Haines Avenue project has very strong capacity against fatigue cracking. Even for the 5 in (127 mm) slabs, the fatigue damage in the design period is only 4.7 percent (page 63). On the other hand, thinner FRC sections have greater elastic deformation. The increased flexibility due to reduction of thickness makes the FRC pavements vulnerable to erosion, and other distresses near transverse joints, which control the FRC pavement design.

9. Comparison of SFRC with Plain Concrete in Thickness Design

If the original PCA method is used to design a plain PCC pavement under the same traffic loads, the only difference in the design procedure is the fatigue analysis.

Figure 9.1d on page 65 shows a worksheet of calculations. Columns 1 and 2 are the same as those in Fig. 9.1a. The equivalent stresses (items 8 & 11) are obtained from Table 9.2b (page 67) based on a slab thickness of 7 in (178 mm) and k value of 134 pci (36.4 MPa/m). The stress ratio factors (items 9 & 12) are obtained by dividing the equivalent stresses with the 28-day modulus of rupture which is estimated as 650 psi (4.48 MPa) for the normal pavement concrete in South Dakota (office practice of Materials and Surfacing, SD DOT). The allowable repetitions (column 4) are directly determined from a PCA design chart (Fig. 9.2c on page 72). The fatigue percentages (column 5) are obtained by dividing column 3 with column 4 and multiplying by 100. The sum of fatigue percentages of all single-axle and tandem-axle loads is entered at the bottom of column 5. The erosion factors (items 10 and 13) are obtained from Table 9.3b on page 68 and the allowable repetitions for erosion analysis (column 6) from Fig. 9.2a on page 70. The erosion damage percentages (column 7) are obtained by dividing column 3 with column 6 and multiplying by 100. The total erosion damage is summed up at the bottom of column 7.

The calculation shows that 7.0 in (178 mm) normal plain concrete pavement is adequate for the design conditions with fatigue and erosion damage ratios of 56.7 % and 47.3 %, respectively. The calculations in Fig. 9.1e on page 66 indicate that 6.5 in. is not adequate because of excessive fatigue consumption (253 %). The plain concrete pavement design is controlled by the fatigue cracking in contrast with the SFRC pavement design which is controlled by erosion. If dowels are used for the plain concrete pavement, the required thickness remains the same because the dowels added can only reduce the erosion damage which does not control the design. For the traffic condition of this example, the design thickness of concrete pavement is reduced about 20 % from 7.0 in (178 mm) to 5.5 in (140 mm) due to the fiber reinforcement.

Calculation of FRC Pavement Thickness

Project: Haines Ave. from I-90 to E. North St. in Rapid City, four-lane arterial street
Trial thickness: 6.0 in. Doweled joint: No *
Subbase-subgrade: k = 134 pci Concrete shoulder: Yes
Modulus of rupture: MR_{28} = 775 psi Design period: 20 years
Strength gain factor: F_A = 1.38 Load Safety factor: LSF = 1.1
Static flexural strength: $S_c = 0.85F_A(MR_{28})$ = 909 psi

Axle load kips	multiplied by LSF	Expected Repetitions	Fatigue analysis				Erosion analysis	
			edge stress	stress ratio	allowable repetitions	fatigue percent	allowable repetitions	damage percent
1	2	3	4	5	6	7	8	9
Single Axles			10. Equivalent stress = 311 psi				11. Erosion factor = 2.73	
28	30.8	2040	515	0.567	unlimited	0.0	88000	2.3
26	28.6	4080	481	0.529	unlimited	0.0	140000	2.9
24	26.4	5110					210000	2.4
22	24.2	8180					380000	2.2
20	22.0	11240					730000	1.5
18	19.8	12250					1800000	0.7
16	17.6	39900					7000000	0.6
14	15.4	44980					unlimited	0.0
12	13.2	159500						
9	9.9	330300						
Tandem Axles			12. Equivalent stress = 262 psi				13. Erosion factor = 2.78	
52	57.2	1010	405	0.445	unlimited	0.0	100000	1.0
46	50.6	6130					210000	2.9
44	48.4	9200					270000	3.4
42	46.2	13300					390000	3.4
40	44.0	7170					530000	1.4
38	41.8	14310					800000	1.8
36	39.6	14310					1300000	1.1
34	37.4	18410					2000000	0.9
32	35.2	16360					3500000	0.5
30	33.0	21480					7000000	0.3
28	30.8	54200					28000000	0.2
22	24.2	101200					unlimited	0.0
16	17.6	181000						
					Total	0.0	Total	29.5

* Joints are saw cut without dowels but steel fibers enhance load transfer over the joints.

Figure 9.1a Worksheet for Sample Problem (h = 6 in)

Calculation of FRC Pavement Thickness

Project: Haines Ave. from I-90 to E. North St. in Rapid City, four-lane arterial street

Trial thickness: 5.0 in. Doweled joint: No *

Subbase-subgrade: k = 134 pci Concrete shoulder: Yes

Modulus of rupture: MR_{28} = 775 psi Design period: 20 years

Strength gain factor: F_A = 1.38 Load Safety factor: LSF = 1.1

Static flexural strength: $S_c = 0.85F_A(MR_{28})$ = 909 psi

Axle load kips	Multiplied by LSF	Expected Repetitions	Fatigue analysis				Erosion analysis	
			edge stress	stress ratio	allowable repetitions	fatigue percent	allowable repetitions	damage percent
1	2	3	4	5	6	7	8	9
Single Axles			10. Equivalent stress = 397 psi			11. Erosion factor = 2.96		
28	30.8	2040	658	0.724	48540	4.2	21000	9.7
26	28.6	4080	614	0.675	759000	0.5	30000	13.6
24	26.4	5110	569	0.626	unlimited	0.0	48000	10.6
22	24.2	8180					79000	10.4
20	22.0	11240					140000	8.0
18	19.8	12250					260000	4.7
16	17.6	39900					600000	6.7
14	15.4	44980					1800000	2.5
12	13.2	159500					10000000	1.6
9	9.9	330300					unlimited	0.0
Tandem Axles			12. Equivalent stress = 331 psi			13. Erosion factor = 2.95		
52	57.2	1010	512	0.563	unlimited	0.0	30000	3.4
46	50.6	6130					64000	9.6
44	48.4	9200					82000	11.2
42	46.2	13300					110000	12.1
40	44.0	7170					150000	4.8
38	41.8	14310					200000	7.2
36	39.6	14310					270000	5.3
34	37.4	18410					420000	4.4
32	35.2	16360					650000	2.5
30	33.0	21480					1000000	2.1
28	30.8	54200					1800000	3.0
22	24.2	101200					50000000	0.2
16	17.6	181000					unlimited	0.0
					Total	4.7	Total	133.6

* Joints are saw cut without dowels but steel fibers enhance load transfer over the joints.

Figure 9.1b Worksheet for Sample Problem (h = 5 in)

Calculation of FRC Pavement Thickness

Project: Haines Ave. from I-90 to E. North St. in Rapid City, four-lane arterial street

Trial thickness: 5.5 in. | Doweled joint: No *

Subbase-subgrade: k = 134 pci | Concrete shoulder: Yes

Modulus of rupture: MR_{28} = 775 psi | Design period: 20 years

Strength gain factor: F_A = 1.38 | Load Safety factor: LSF = 1.1

Static flexural strength: $S_c = 0.85F_A(MR_{28})$ = 909 psi

Axle load kips	Multiplied by LSF	Expected Repetitions	Fatigue analysis				Erosion analysis	
			edge stress	stress ratio	allowable repetitions	fatigue percent	allowable repetitions	damage percent
1	2	3	4	5	6	7	8	9
Single Axles			10. Equivalent stress = 350 psi				11. Erosion factor = 2.84	
28	30.8	2040	580	0.638	unlimited	0.0	42000	4.9
26	28.6	4080	541	0.595	unlimited	0.0	64000	6.4
24	26.4	5110					101000	5.1
22	24.2	8180					170000	4.8
20	22.0	11240					310000	3.6
18	19.8	12250					640000	1.9
16	17.6	39900					1700000	2.3
14	15.4	44980					6500000	0.7
12	13.2	159500					unlimited	0.0
9	9.9	330300						
Tandem Axles			12. Equivalent stress = 293 psi				13. Erosion factor = 2.86	
52	57.2	1010	453	0.498	unlimited	0.0	59000	1.7
46	50.6	6130					120000	5.1
44	48.4	9200					150000	6.1
42	46.2	13300					200000	6.7
40	44.0	7170					280000	2.6
38	41.8	14310					420000	3.4
36	39.6	14310					550000	2.6
34	37.4	18410					900000	2.0
32	35.2	16360					1500000	1.1
30	33.0	21480					2600000	0.8
28	30.8	54200					5500000	1.0
22	24.2	101200					unlimited	0.0
16	17.6	181000						
					Total	0.0	Total	62.8

* Joints are saw cut without dowels but steel fibers enhance load transfer over the joints.

Figure 9.1c Worksheet for Sample Problem (h = 5.5 in)

Calculation of Plain Concrete Undoweled Pavement Thickness *

Project: Haines Ave. from I-90 to E. North St. in Rapid City, four-lane arterial street
Trial thickness: 7.0 in. Doweled joint: No
Subbase-subgrade: k = 134 pci Concrete shoulder: Yes
Modulus of rupture: MR_{28} = 650 psi Design period: 20 years
Load Safety factor: LSF = 1.1

Axle load kips	multiplied by LSF	Expected Repetitions	Fatigue analysis		Erosion analysis	
			allowable repetitions	fatigue percent	allowable repetitions	damage percent
1	2	3	4	5	6	7
			8. Equivalent stress = 254		10. Erosion factor = 2.76	
Single Axles			9. Stress ratio factor = 0.391			
28	30.8	2040	7000	29.1	75000	2.7
26	28.6	4080	23000	17.7	120000	3.4
24	26.4	5110	80000	6.4	190000	2.7
22	24.2	8180	300000	2.7	320000	2.6
20	22.0	11240	3000000	0.4	630000	1.8
18	19.8	12250	unlimited	0.0	1500000	0.8
16	17.6	39900			4300000	0.9
14	15.4	44980			41000000	0.1
12	13.2	159500			unlimited	0.0
9	9.9	330300				
			11. Equivalent stress = 216		13. Erosion factor = 2.86	
Tandem Axles			12. Stress ratio factor = 0.332			
52	57.2	1010	350000	0.3	57000	1.8
46	50.6	6130	10000000	0.1	130000	4.7
44	48.4	9200	unlimited	0.0	170000	5.4
42	46.2	13300			200000	6.7
40	44.0	7170			280000	2.6
38	41.8	14310			400000	3.6
36	39.6	14310			580000	2.5
34	37.4	18410			900000	2.0
32	35.2	16360			1500000	1.1
30	33.0	21480			2500000	0.9
28	30.8	54200			5500000	1.0
22	24.2	101200			unlimited	0.0
16	17.6	181000				
			Total	56.7	Total	47.3

* Original PCA method

Figure 9.1d Worksheet for Sample Problem (h = 7 in)

Calculation of Plain Concrete Undoweled Pavement Thickness *

Project: Haines Ave. from I-90 to E. North St. in Rapid City, four-lane arterial street
Trial thickness: 6.5 in. Doweled joint: No
Subbase-subgrade: k = 134 pci Concrete shoulder: Yes
Modulus of rupture: MR_{28} = 650 psi Design period: 20 years
Load Safety factor: LSF = 1.1

Axle load kips	multiplied by LSF	Expected Repetitions	Fatigue analysis		Erosion analysis	
			allowable repetitions	fatigue percent	allowable repetitions	damage percent
1	2	3	4	5	6	7
			8. Equivalent stress = 280		10. Erosion factor = 2.84	
Single Axles			9. Stress ratio factor = 0.431			
28	30.8	2040	1600	127.5	43000	4.7
26	28.6	4080	5000	81.6	64000	6.4
24	26.4	5110	20000	25.6	100000	5.1
22	24.2	8180	70000	11.7	170000	4.8
20	22.0	11240	300000	3.7	320000	3.5
18	19.8	12250	3600000	0.3	650000	1.9
16	17.6	39900	unlimited	0.0	1700000	2.3
14	15.4	44980			7000000	0.6
12	13.2	159500			unlimited	0.0
9	9.9	330300				
			11. Equivalent stress = 237		13. Erosion factor = 2.92	
Tandem Axles			12. Stress ratio factor = 0.365			
52	57.2	1010	85000	1.2	40000	2.5
46	50.6	6130	700000	0.9	82000	7.5
44	48.4	9200	2000000	0.5	105000	8.8
42	46.2	13300	unlimited	0.0	140000	9.5
40	44.0	7170			190000	3.8
38	41.8	14310			280000	5.1
36	39.6	14310			380000	3.8
34	37.4	18410			550000	3.3
32	35.2	16360			850000	1.9
30	33.0	21480			1500000	1.4
28	30.8	54200			2600000	2.1
22	24.2	101200			unlimited	0.0
16	17.6	181000				
			Total	253.0	Total	79.0

* Original PCA method

Figure 9.1e Worksheet for Sample Problem (h =6.5 in)

Table 9.2a Equivalent Stresses for Slabs without Concrete Shoulders (Single Axle/Tandem Axle) (After PCA 1984)

Slab thickness in.	k of subgrade-subbase, pci						
	50	100	150	200	300	500	700
4 4.5	825/679 699/586	726/585 616/500	671/542 571/460	634/516 540/435	584/486 498/406	523/457 448/378	484/443 417/363
5 5.5	602/516 526/461	531/436 464/387	493/399 431/353	467/376 409/331	432/349 379/305	390/321 343/278	363/307 320/264
6 6.5	465/416 417/380	411/348 367/317	382/316 341/286	362/296 324/267	336/271 300/244	304/246 273/220	285/232 256/207
7 7.5	375/349 340/323	331/290 300/268	307/262 279/241	292/244 265/224	271/222 246/203	246/199 224/181	231/186 210/169
8 8.5	331/300 285/281	274/249 252/232	255/223 234/208	242/208 222/193	225/188 206/174	205/167 188/154	192/155 177/143
9 9.5	264/264 245/248	232/218 215/205	216/195 200/183	205/181 190/170	190/163 176/153	174/144 161/134	163/133 151/124
10 10.5	228/235 213/222	200/193 187/183	186/173 174/164	177/160 165/151	164/144 153/136	150/126 140/119	141/117 132/110
11 11.5	200/211 188/201	175/174 165/165	163/155 153/148	154/143 145/136	144/129 135/122	131/113 123/107	123/104 116/98
12 12.5	177/192 168/183	155/158 147/151	144/141 136/135	137/130 129/124	127/116 120/111	116/102 109/97	109/93 103/89
13 13.5	159/176 152/168	139/144 132/138	129/129 122/123	122/119 116/114	113/106 107/102	103/93 98/89	97/85 92/81
14	144/162	125/133	116/118	110/109	102/98	93/85	88/87

Table 9.2b Equivalent Stresses for Slabs with Concrete Shoulders (Single Axle/Tandem Axle) (After PCA 1984)

Slab thickness in.	k of subgrade-subbase, pci						
	50	100	150	200	300	500	700
4 4.5	640/534 547/461	559/468 479/400	517/439 444/372	489/422 421/356	452/403 390/388	409/388 355/322	383/384 333/316
5 5.5	475/404 418/360	417/349 368/309	387/323 342/285	367/308 324/271	341/290 302/254	311/274 276/238	294/267 261/231
6 6.5	372/325 344/295	327/277 294/251	304/255 274/230	289/241 260/218	270/225 243/203	247/210 223/188	234/203 212/180
7 7.5	302/270 275/250	266/230 243/211	248/210 226/193	236/198 215/182	220/184 201/168	203/170 185/155	192/162 176/148
8 8.5	252/232 232/216	222/196 205/182	207/179 191/166	197/168 182/156	185/155 170/144	170/142 157/131	162/135 150/125
9 9.5	215/202 200/190	190/171 176/160	177/155 164/146	169/146 157/137	158/134 147/126	146/122 136/114	139/116 129/108
10 10.5	186/179 174/170	164/151 154/143	153/137 144/130	146/129 137/121	138/118 128/111	127/107 119/101	121/101 113/95
11 11.5	164/161 154/153	144/135 136/128	135/123 127/117	129/115 121/109	120/105 113/100	112/95 105/90	106/90 100/85
12 12.5	145/146 137/139	128/122 121/117	120/111 113/106	114/104 108/99	107/95 101/91	99/86 94/82	95/81 90/77
13 13.5	130/133 124/127	115/112 109/107	107/101 102/97	102/95 97/91	96/86 91/83	89/78 85/74	85/73 81/70
14	118/122	104/103	97/93	93/87	87/79	81/71	77/67

Table 9.3a Erosion Factors for Slabs with Doweled Joints & Concrete Shoulders (Single Axle/Tandem Axle) (After PCA 1984)

Slab thickness in.	k of subgrade-subbase, pci					
	50	100	200	300	500	700
4 4.5	3.28/3.30 3.13/3.19	3.24/3.20 3.09/3.08	3.21/3.13 3.06/3.00	3.19/3.10 3.04/2.96	3.15/3.09 3.01/2.93	3.12/3.08 2.98/2.91
5 5.5	3.01/3.09 2.90/3.01	2.97/2.98 2.85/2.89	2.93/2.89 2.81/2.79	2.90/2.84 2.79/2.74	2.87/2.79 2.74/2.68	2.85/2.77 2.73/2.65
6 6.5	2.79/2.93 2.70/2.86	2.75/2.82 2.65/2.75	2.70/2.71 2.61/2.63	2.68/2.65 2.58/2.57	2.65/2.58 2.55/2.50	2.62/2.54 2.52/2.45
7 7.5	2.61/2.79 2.53/2.73	2.56/2.68 2.48/2.62	2.52/2.56 2.44/2.50	2.49/2.50 2.41/2.44	2.46/2.42 2.38/2.36	2.43/2.38 2.35/2.31
8 8.5	2.46/2.68 2.39/2.62	2.41/2.56 2.34/2.51	2.36/2.44 2.29/2.39	2.33/2.38 2.26/2.32	2.30/2.30 2.22/2.24	2.27/2.24 2.20/2.18
9 9.5	2.32/2.57 2.26/2.52	2.27/2.46 2.21/2.41	2.22/2.34 2.16/2.29	2.19/2.27 2.13/2.22	2.16/2.19 2.09/2.14	2.13/2.13 2.07/2.08
10 10.5	2.20/2.47 2.15/2.43	2.15/2.36 2.09/2.32	2.10/2.25 2.04/2.20	2.07/2.18 2.01/2.14	2.03/2.09 1.97/2.05	2.01/2.03 1.95/1.99
11 11.5	2.10/2.39 2.05/2.35	2.04/2.28 1.99/2.24	1.99/2.16 1.93/2.12	1.95/2.09 1.90/2.05	1.92/2.01 1.87/1.97	1.89/1.95 1.84/1.91
12 12.5	2.00/2.31 1.95/2.27	1.94/2.20 1.89/2.16	1.88/2.09 1.84/2.05	1.85/2.02 1.81/1.98	1.82/1.93 1.77/1.89	1.79/1.87 1.74/1.84
13 13.5	1.91/2.23 1.86/2.20	1.82/2.13 1.81/2.09	1.79/2.01 1.75/1.98	1.76/1.95 1.72/1.91	1.72/1.86 1.68/1.83	1.70/1.80 1.65/1.77
14	1.82/2.17	1.76/2.06	1.71/1.96	1.67/1.88	1.64/1.80	1.61/1.74

Table 9.3b Erosion Factors for Slabs with Aggregate-Interlock Joints & Concrete Shoulders (Single Axle/Tandem Axle) (After PCA 1984)

Slab thickness in.	k of subgrade-subbase, pci					
	50	100	200	300	500	700
4 4.5	3.46/3.49 3.23/3.39	3.42/3.39 3.28/3.28	3.38/3.32 3.24/3.19	3.36/3.29 3.22/3.16	3.32/3.26 3.19/3.12	3.28/3.24 3.15/3.09
5 5.5	3.20/3.30 3.10/3.22	3.16/3.18 3.05/3.10	3.12/3.09 3.01/3.00	3.10/3.05 2.99/2.95	3.07/3.00 2.96/2.90	3.04/2.97 2.93/2.86
6 6.5	3.00/3.15 2.91/3.08	2.95/3.02 2.86/2.96	2.90/2.92 2.81/2.85	2.88/2.87 2.79/2.79	2.86/2.81 2.76/2.73	2.83/2.77 2.74/2.68
7 7.5	2.83/3.02 2.76/2.91	2.77/2.90 2.70/2.84	2.73/2.78 2.65/2.72	2.70/2.72 2.62/2.66	2.68/2.66 2.60/2.59	2.65/2.61 2.57/2.54
8 8.5	2.69/2.92 2.63/2.88	2.63/2.79 2.56/2.74	2.57/2.67 2.51/2.62	2.55/2.61 2.48/2.55	2.52/2.53 2.45/2.48	2.50/2.48 2.43/2.43
9 9.5	2.57/2.83 2.51/2.79	2.50/2.70 2.44/2.65	2.44/2.57 2.38/2.53	2.42/2.51 2.36/2.46	2.39/2.43 2.33/2.38	2.36/2.38 2.30/2.33
10 10.5	2.46/2.75 2.41/2.72	2.39/2.61 2.33/2.58	2.33/2.49 2.27/2.45	2.30/2.42 2.24/2.38	2.27/2.34 2.21/2.30	2.24/2.28 2.19/2.24
11 11.5	2.36/2.68 2.32/2.65	2.28/2.54 2.24/2.51	2.22/2.41 2.17/2.38	2.19/2.34 2.14/2.31	2.16/2.26 2.11/2.22	2.14/2.20 2.09/2.16
12 12.5	2.28/2.62 2.24/2.59	2.19/2.48 2.15/2.45	2.13/2.34 2.09/2.31	2.10/2.27 2.05/2.24	2.06/2.19 2.02/2.15	2.04/2.13 1.99/2.10
13 13.5	2.20/2.56 2.16/2.53	2.11/2.42 2.08/2.39	2.04/2.28 2.00/2.25	2.01/2.21 1.97/2.18	1.98/2.12 1.93/2.09	1.95/2.06 1.91/2.03
14	2.13/2.51	2.04/2.36	1.97/2.23	1.93/2.15	1.89/2.06	1.87/2.00

Table 9.3c Erosion Factors for Slabs with Doweled Joints & No Concrete Shoulders (Single Axle/Tandem Axle) (After PCA 1984)

Slab thickness in.	k of subgrade-subbase, pci					
	50	100	200	300	500	700
4 4.5	3.74/3.83 3.59/3.70	3.73/3.79 3.57/3.65	3.72/3.75 3.56/3.61	3.71/3.73 3.55/3.58	3.70/3.70 3.54/3.55	3.68/3.67 3.52/3.53
5 5.5	3.45/3.58 3.33/3.47	3.43/3.52 3.31/3.41	3.42/3.48 3.29/3.36	3.41/3.45 3.28/3.33	3.40/3.42 3.27/3.30	3.38/3.40 3.26/3.28
6 6.5	3.22/3.38 3.11/3.29	3.19/3.31 3.09/3.22	3.18/3.26 3.07/3.16	3.17/3.23 3.06/3.13	3.15/3.20 3.05/3.10	3.14/3.17 3.03/3.10
7 7.5	3.02/3.21 2.93/3.14	2.99/3.14 2.91/3.06	2.97/3.08 2.88/3.00	2.96/3.05 2.87/2.97	2.95/3.01 2.86/2.93	2.94/2.98 2.84/2.90
8 8.5	2.85/3.07 2.77/3.01	2.82/2.99 2.74/2.93	2.80/2.93 2.72/2.86	2.79/2.89 2.71/2.82	2.77/2.85 2.69/2.78	2.76/2.82 2.68/2.75
9 9.5	2.70/2.96 2.63/2.90	2.67/2.87 2.60/2.81	2.65/2.80 2.58/2.74	2.63/2.76 2.56/2.70	2.62/2.71 2.55/2.65	2.61/2.68 2.54/2.62
10 10.5	2.56/2.85 2.50/2.81	2.54/2.76 2.47/2.71	2.51/2.68 2.45/2.63	2.50/2.64 2.44/2.59	2.48/2.59 2.42/2.54	2.47/2.56 2.41/2.51
11 11.5	2.44/2.76 2.38/2.72	2.42/2.67 2.36/2.62	2.39/2.58 2.33/2.54	2.38/2.54 2.32/2.49	2.36/2.49 2.30/2.44	2.35/2.45 2.90/2.40
12 12.5	2.33/2.68 2.28/2.64	2.30/2.58 2.25/2.54	2.28/2.49 2.23/2.45	2.26/2.44 2.21/2.40	2.25/2.39 2.19/2.35	2.23/2.36 2.18/2.31
13 13.5	2.23/2.61 2.18/2.57	2.20/2.50 2.15/2.47	2.18/2.41 2.13/2.37	2.16/2.36 2.11/2.32	2.14/2.30 2.09/2.26	2.13/2.27 2.08/2.23
14	2.13/2.54	2.11/2.43	2.08/2.34	2.07/2.29	2.05/2.23	2.03/2.19

Table 9.3d Erosion Factors for Slabs with Aggregate-Interlock Joints & No Concrete Shoulders (Single Axle/Tandem Axle) (After PCA 1984)

Slab thickness in.	k of subgrade-subbase, pci					
	50	100	200	300	500	700
4 4.5	3.94/4.03 3.79/3.91	3.91/3.95 3.76/3.82	3.88/3.89 3.73/3.75	3.86/3.86 3.71/3.72	3.82/3.83 3.68/3.68	3.77/3.80 3.64/3.65
5 5.5	3.66/3.81 3.54/3.72	3.63/3.72 3.51/3.62	3.60/3.64 2.48/3.53	3.58/3.60 3.46/3.49	3.55/3.55 3.43/3.44	3.52/3.52 3.41/3.40
6 6.5	3.44/3.64 3.34/3.56	3.40/3.53 3.30/3.46	3.37/3.44 3.26/3.36	3.35/3.40 3.25/3.31	3.32/3.34 3.22/3.23	3.30/3.30 3.20/3.21
7 7.5	3.26/3.49 3.18/3.43	3.21/3.39 3.13/3.32	3.17/3.29 3.09/3.22	3.15/3.24 3.07/2.17	3.13/3.17 3.04/3.10	3.11/3.13 3.02/3.06
8 8.5	3.11/3.37 3.04/3.32	3.05/3.26 2.98/3.21	3.01/3.16 2.93/3.10	2.99/3.10 2.91/3.04	2.96/3.03 2.88/2.97	2.94/2.99 2.87/2.93
9 9.5	2.98/3.27 2.92/3.22	2.91/3.16 2.85/3.11	2.86/3.05 2.80/3.00	2.84/2.99 2.77/2.94	2.81/2.92 2.75/2.86	2.79/2.87 2.73/2.81
10 10.5	2.86/3.18 2.81/3.14	2.79/3.06 2.74/3.02	2.74/2.95 2.68/2.91	2.71/2.89 2.65/2.84	2.68/2.81 2.62/2.76	2.66/2.76 2.60/2.72
11 11.5	2.77/3.10 2.72/3.06	2.69/2.98 2.64/2.94	2.63/2.86 2.58/2.82	2.60/2.80 2.55/2.76	2.57/2.72 2.51/2.68	2.54/2.67 2.49/2.63
12 12.5	2.68/3.03 2.64/2.99	2.60/2.90 2.55/2.87	2.53/2.78 2.48/2.75	2.50/2.72 2.45/2.68	2.46/2.64 2.41/2.60	2.44/2.59 2.39/2.55
13 13.5	2.60/2.96 2.56/2.93	2.51/2.83 2.47/2.80	2.44/2.71 2.40/2.68	2.40/2.65 2.36/2.61	2.36/2.56 2.32/2.53	2.34/2.51 2.30/2.48
14	2.53/2.90	2.44/2.77	2.36/2.65	2.32/2.58	2.28/2.50	2.25/2.44

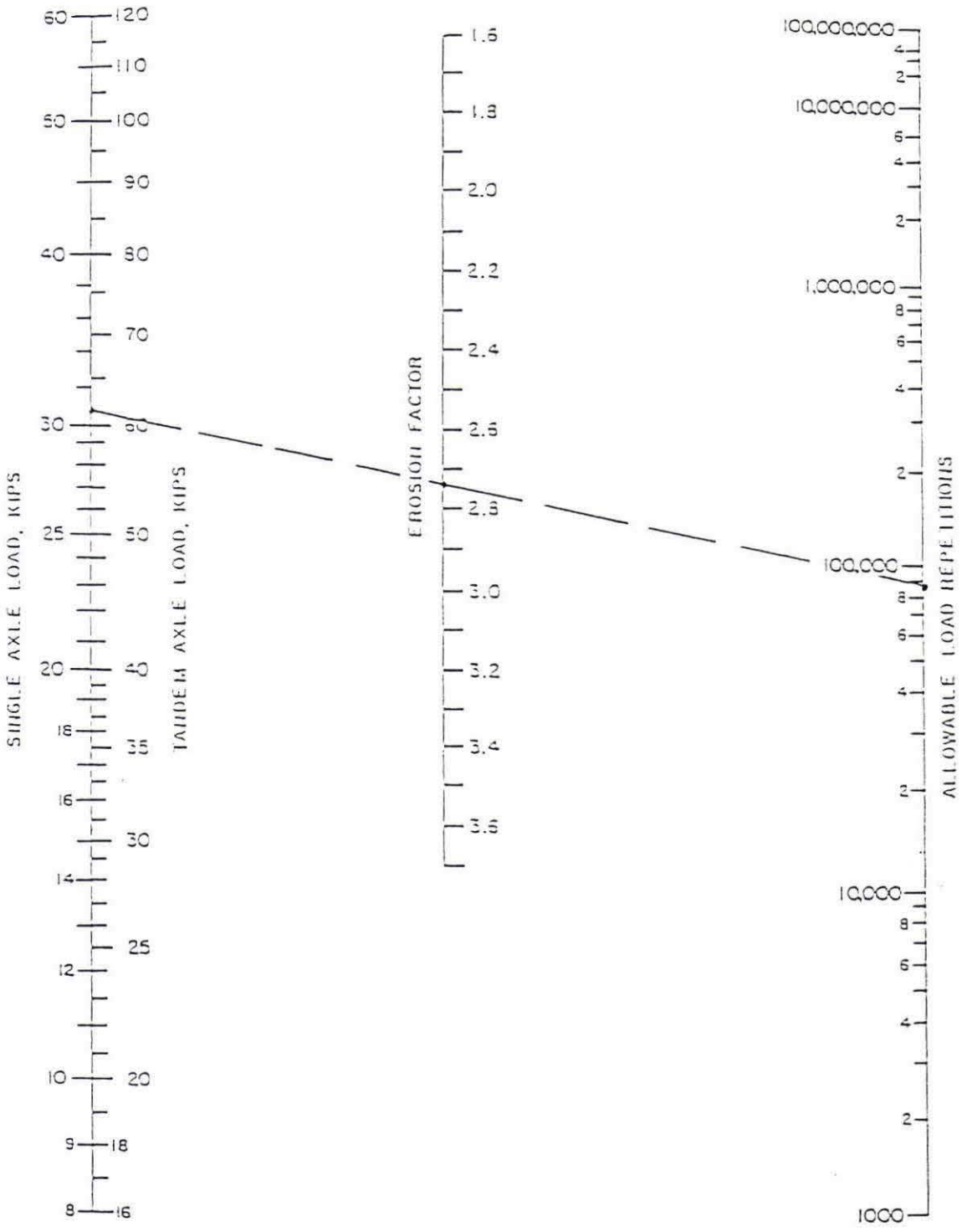

Figure 9.2a Allowable load repetitions based on erosion factor (with concrete shoulder), (After PCA 1984)

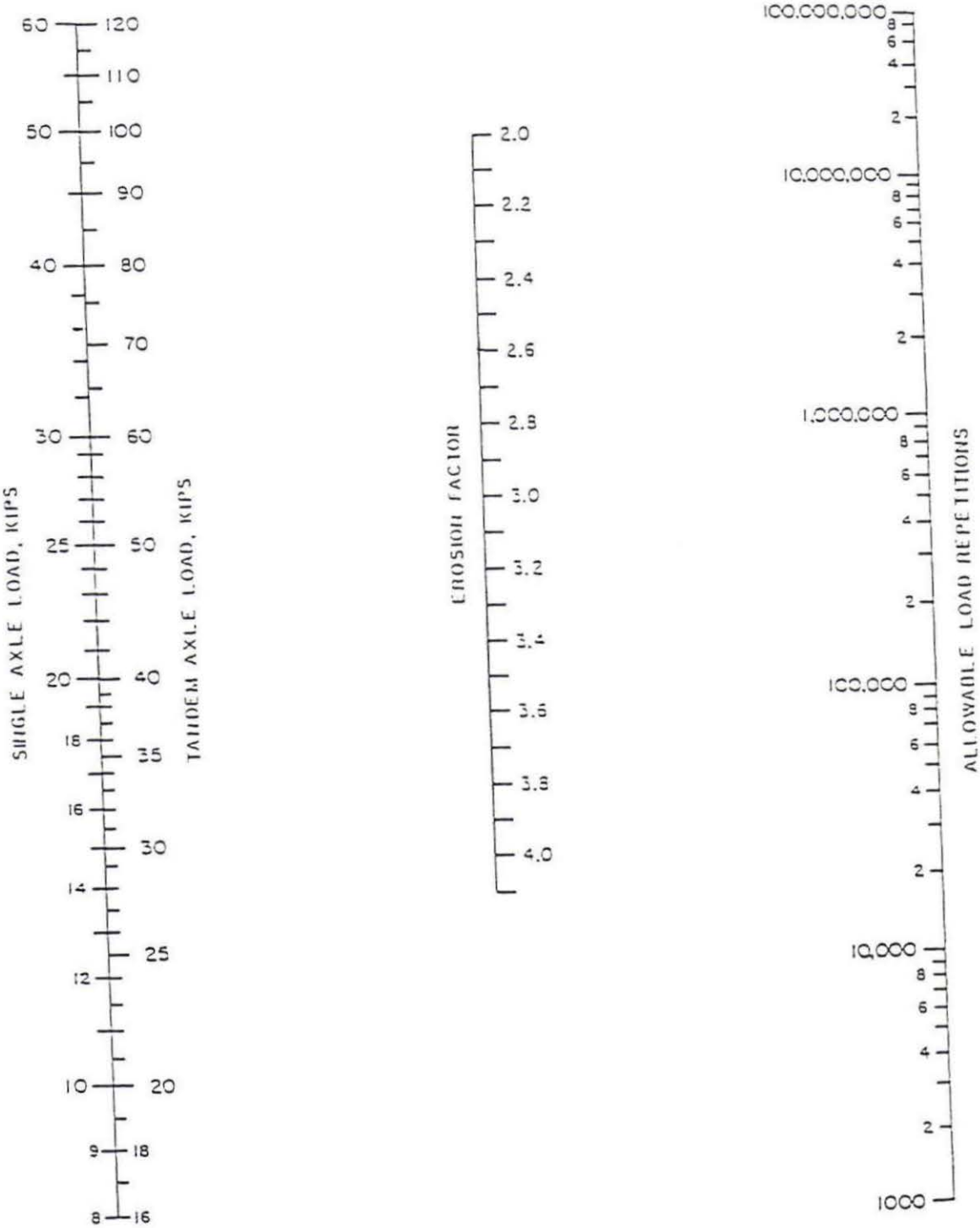

Figure 9.2b Allowable load repetitions based on erosion factor (without concrete shoulder), (After PCA 1984)

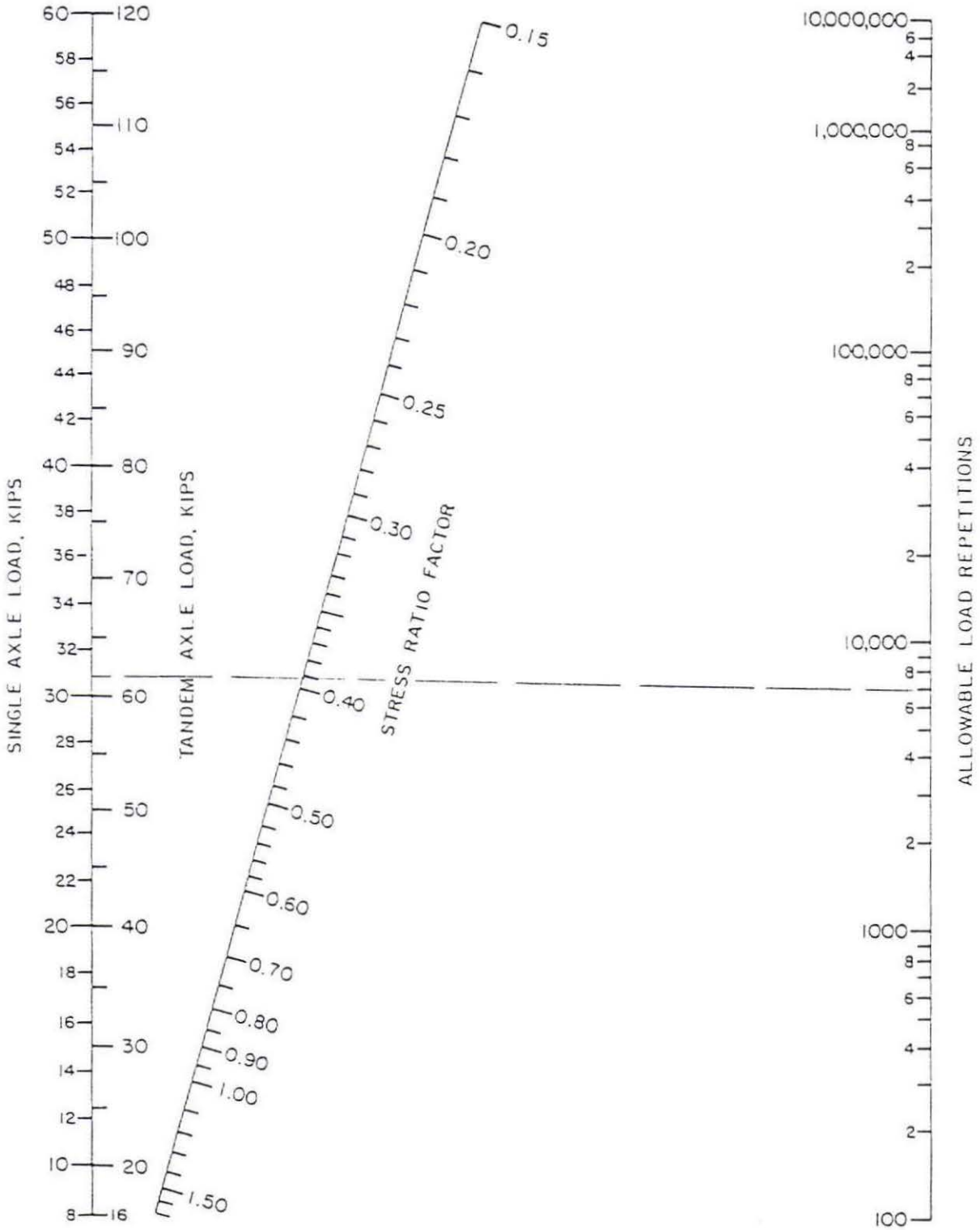

Figure 9.2c Allowable load repetitions based on stress ratio factor (After PCA 1984)

10. FIELD INSPECTION OF SFRC PAVEMENT (HAINES AVENUE)

Task 6: The task of this chapter is to report a field survey of the SFRC pavements on Haines Avenue. The survey was conducted in accordance with "Distress Identification Manual for the Long-Term Pavement Performance Project" [30] after the SFRC test sections had been in service for seven years.

10.1 Construction Condition and Previous Inspections [2]

The south-bound lanes of the project were constructed on June 1, 1988, when the weather conditions were excellent for concreting (62° F or 18.3° C and 55 % relative humidity). Unfortunately, the north-bound lanes were placed under a hot and dry weather condition (40.6° C or 105° F and 10 % relative humidity) on June 7, 1988. Several inspections were conducted after the construction on June 23, June 30, July 7, and July 25 in 1988. A total of 30 cracks were reported on the north-bound lanes from station 36+00 to station 50+00 which were constructed after 11 am, when the temperature exceeded 37.8° C (100° F). The length of theses cracks varied from 127 mm to 1524 mm (5 to 60 in) and the width varied from 0.20 to 0.40 mm (0.008 to 0.016 in). Most cracks occurred near intersections of longitudinal construction joints (center line of roadway) and transverse contraction joints. Twenty-nine cracks were in the plain concrete section. Only one crack was in the 5-inch SFRC section near station 36+30.

These cracks were originally repaired with small patches about 50 to 100 mm (2 to 4 in) wide and 305 to 1830 mm (1 to 6 ft) long in 1988. Because these small patches had been debonding, they were replaced by 27 full-depth concrete patches during

March-April 1990. Only one concrete patch was in the SFRC section (Figure 10.1a)

During the inspection on September 4, 1992, three new cracks were found in the SFRC section on the north bound driving lane (Figure 10.1c, cracks No.1, No. 2 & No.3). On a subsequent inspection on March 4, 1993, crack No. 4 was reported at the same station but on the south bound lane.

10.2 Recent Inspection of SFRC Pavement

The SFRC pavement was inspected again on may 21, 1995. Crack No. 5 was found in the 127 mm (5 in) SFRC section. It was found that the length of crack No. 3 had increased from previous reported 1525 mm (5 ft) to 2440 (8 ft). However, there was no widening of the old cracks and most of them were well-sealed. The concrete patch on the north bound passing lane is in good condition. A spall was found at transverse joint on the south bond passing lane opposite the patch. Visible faulting of transverse joint was found on the north bound lanes adjacent to slab thickness transition section (Figures 10.1a and 10.1d). It should be noticed that the SFRC was used actually beyond the designated sections on the north bound lanes, passing the transition section and extending to about station 37+00. The distresses in the SFRC pavement were measured in accordance with the "Distress Identification Manual for the Long-Term Pavement Performance Project" [30] as follows:

Patch - The plain concrete patch is in good condition without cracking or faulting. The patch is 914 mm (3'- 0") wide and 2159 mm (7'- 1") long. The location of the patch is shown in Figures 10.1a and 10.1b.

Spalling of transverse joint - The spall is categorized as at "low severity level" because it is less than 75 mm (3 in) wide. The length of the spall is 330 mm (13 in), which is less 10 % of the total length of the joint. The location of the spall is shown in Figures 10.1a and 10.1b.

Cracking near joints - The dimensions of the cracks are listed in Table 10.1. The locations are shown in Figures 10.1a and 10.1c. Only crack No. 1 can be measured by a plug gage. The severity level of these cracks is "low" because the crack widths are less than 3 mm (0.125 in) or well-sealed. There is no spalling or faulting in association with the cracks.

Table 10.1 Crack Dimensions

Crack Number	Crack Length		Crack Width	
	mm	in	mm	in
1	940	37	0.25	0.01
2	635	25	*	*
3	2438	96	*	*
4	762	30	*	*
5	1067	42	*	*

* Well-sealed crack and the width cannot be measured.

Faulting of transverse joint - A visible fault occurs at the north bound driving lane and passing lane. The leading slab is 0.5 inch (13 mm) lower than the approach slab (positive faulting). The location and a section view of the fault are shown in Figures 10.1a and 10.1d.

No distresses have been found in the 6-inch SFRC section either on the north bound

or south bound lanes. No transverse fatigue cracks have appeared in any section of SFRC pavement so far.

Both the theoretical analysis and the field inspection indicate that the SFRC used in the Haines Avenue project is very strong against transverse fatigue cracking, one of common distresses of rigid pavements. However, when the thickness of slab is reduced, the deflection at joints becomes the major concern of FRC pavement design. Excessive deflection at joints can cause plastic deformation of the subgrade which in turn result in faulting or voids under the slab near the joints. The vertical movement at joints creates chances for infiltration of incompressible material into joints, which causes compressive stresses and leads to spalling and cracking near joints. Because the PCA erosion criterion is based on the critical deflection and pressure under concrete slabs near joints, it also provides a control over the other distresses in association with joints.

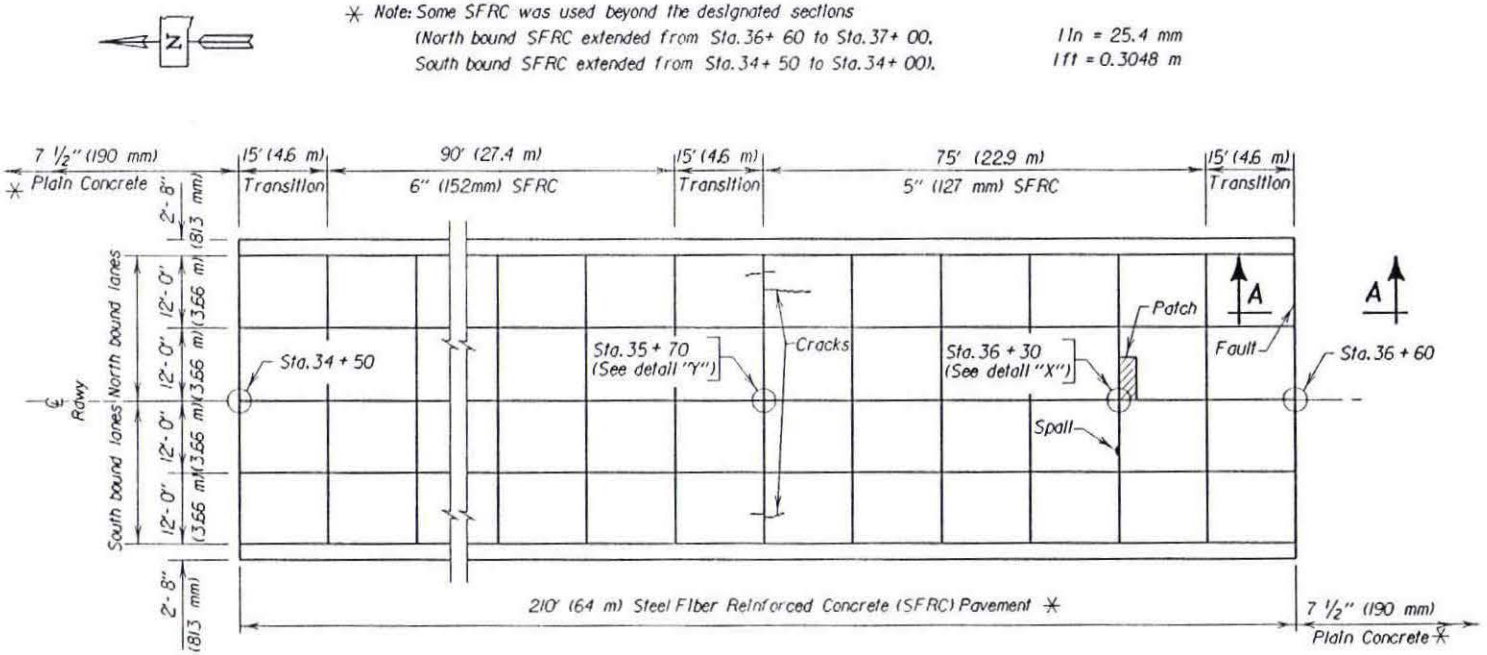

Figure 10.1a Inspection of SFRC Pavement (Haines Avenue, 5/21/1995)

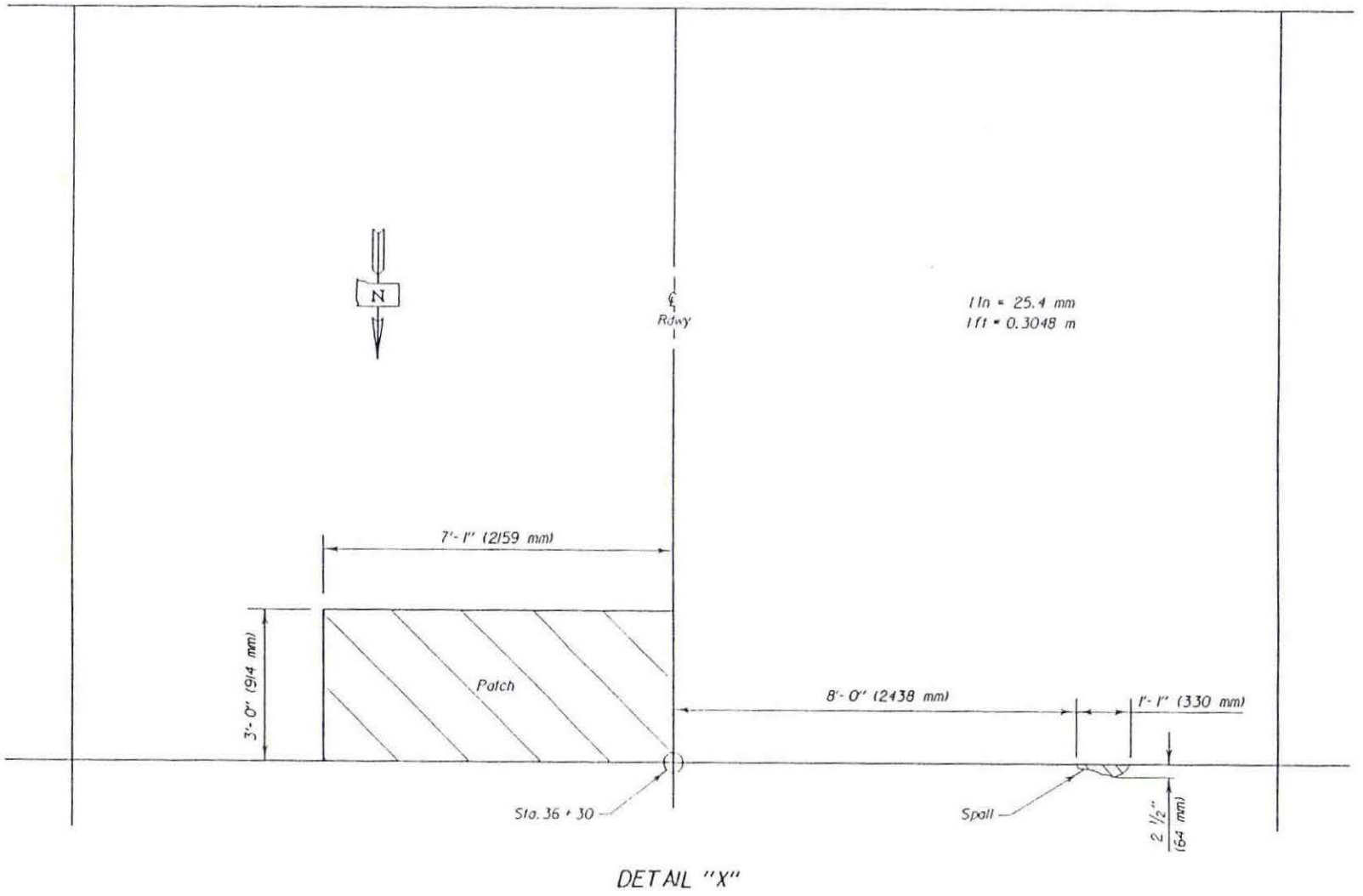

Figure 10.1b Inspection of SFRC Pavement (Detail "X")

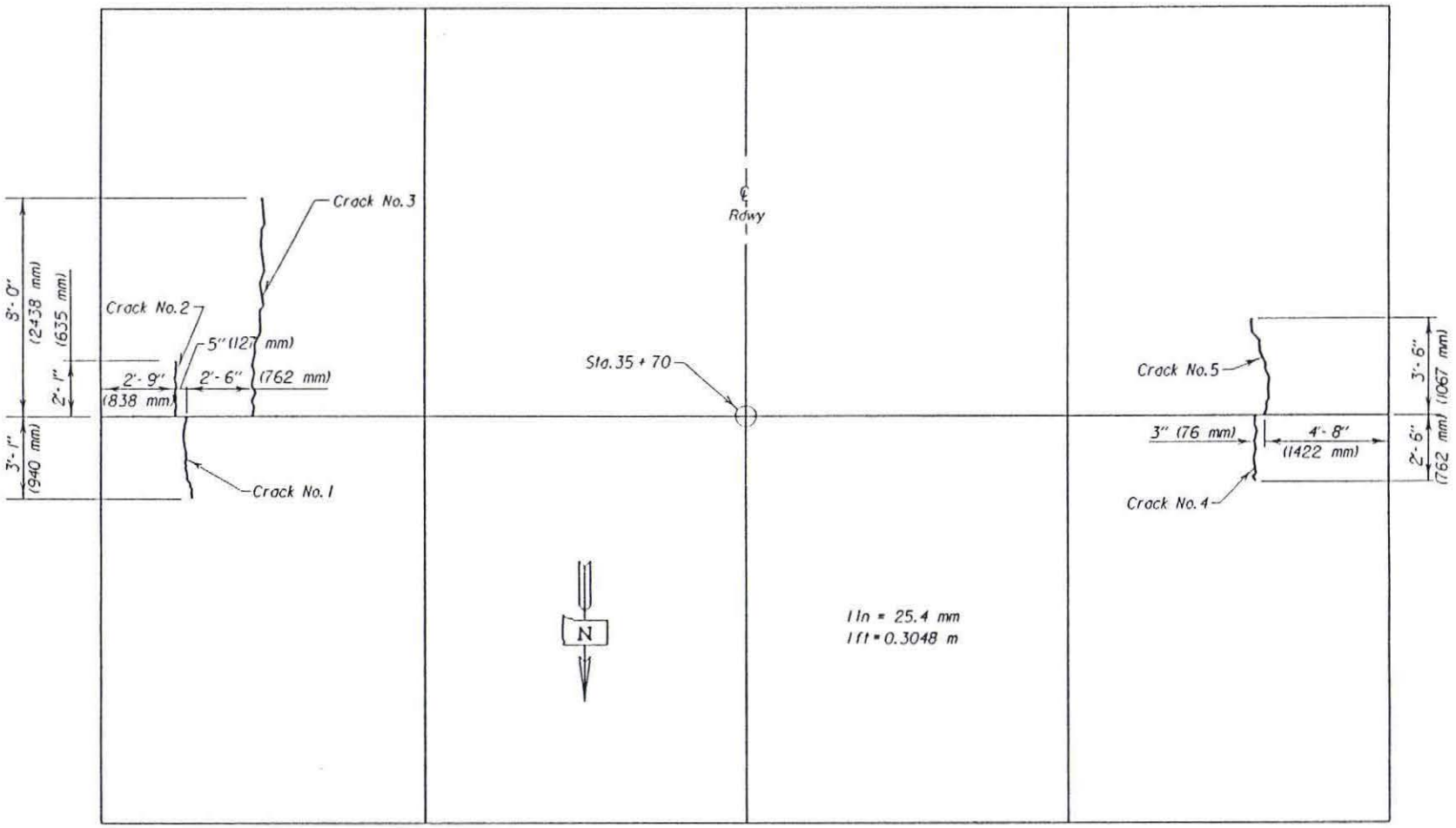

DETAIL "Y"

Figure 10.1c Inspection of SFRC Pavement (Detail "Y")

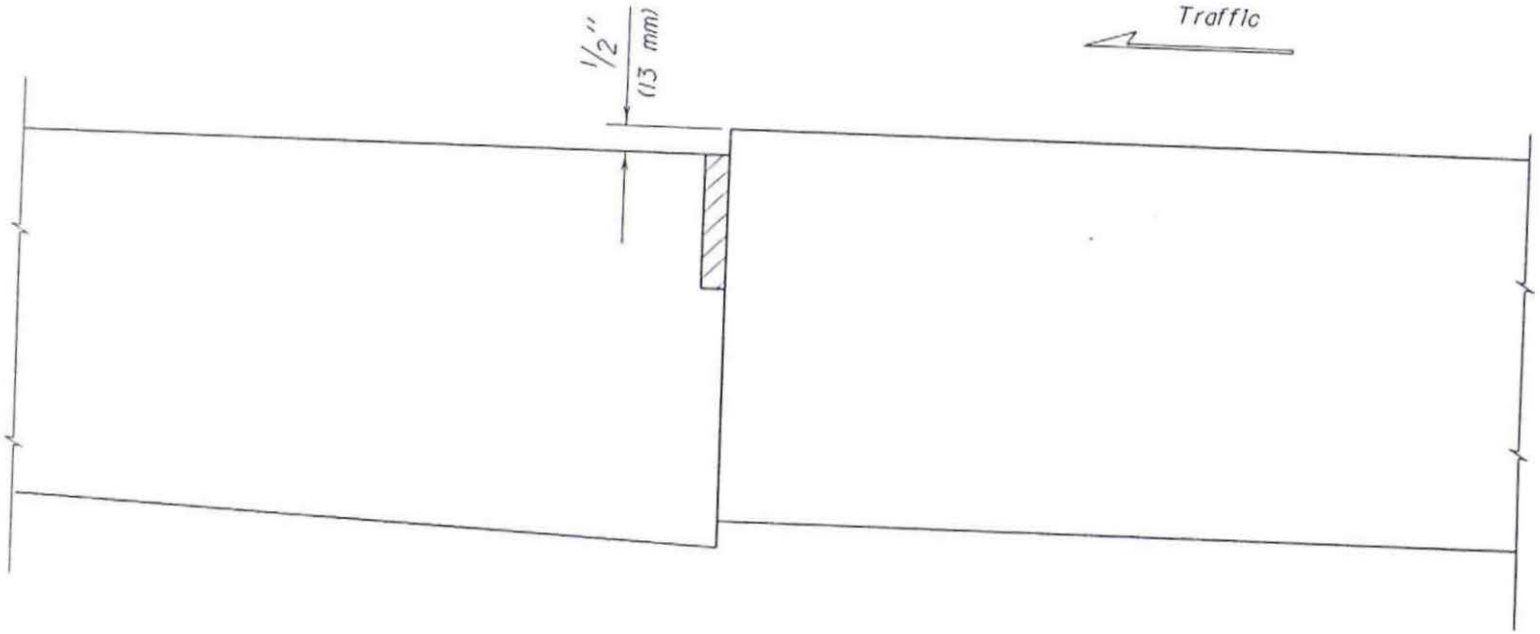

SEC. A - A

Figure 10.1d Inspection of SFRC Pavement (Sec. A - A)

11. CONCLUSIONS AND RECOMMENDATIONS

Conclusions:

1. Fiber reinforced concrete technology can produced a new kind of rigid concrete pavement which possesses fatigue properties different from those assumed in design procedures for conventional concrete pavements.

2. A thickness design method for jointed fiber reinforced concrete pavements is presented. The method is developed by modifying the current PCA "Thickness Design for Concrete Highway and Street Pavements". The modification is based on the fact that the fatigue properties of FRC are different but the elastic properties and stiffness of FRC remain practically the same as plain concrete (the steel fiber content used in this study is 0.5 % by volume). This means the stress and deflection analysis of normal concrete pavements based on small deformation theory of an elastic, medium-thick plate should be also valid for FRC pavements.

3. To recognize the unique fatigue properties of FRC, new endurance limit and fatigue S-N curves must be established from test data of the FRC. It is impractical or impossible to develop a uniform endurance limit and S-N function for all kinds of FRC because the fatigue properties of FRC vary significantly with fiber type, fiber content, aspect ratio, bonding and anchorage features, and mix design. However, test procedures to establish the endurance limit and S-N function of a specific FRC are presented in this study, and the modified design procedure demonstrates how they are used in thickness design of FRC pavements.

4. Both the theoretical analysis and the field inspection of the SFRC pavements on Haines Avenue indicate that the FRC with 0.5 % hooked-end steel fibers is very strong against transverse fatigue cracking. On the other hand, the deflection at joints becomes the major concern of FRC pavement design because of the reduced slab thickness and increased flexibility. The PCA erosion criterion, which is based on critical deflection and subgrade pressure near joints, provide a useful control over erosion and other distresses in association with slab joints.

Recommendations:

1. The thickness design for jointed FRC pavements documented herein is ready for trial implementation. It should be used for the future projects of jointed FRC pavements. The design procedure accounts for the unique fatigue properties of FRC which are different from those assumed in the current design methods for conventional concrete pavements. It is also recommended to keep a good record of traffic data and field inspections of the FRC pavements, so the design method can be improved and calibrated by the actual performance of the FRC pavements when a large collection of performance data are available.

2. For any specific FRC, the material properties such as fatigue endurance limit, fatigue S-N curve, and strength gain factor should be determined from test data before the thickness design. The properties of FRC vary significantly with fiber type, fiber content, aspect ratio, bonding and anchorage features, and mix design.

3. Some measures should be taken to prevent pumping and faulting, because FRC pavements are very strong against transverse fatigue cracking but becomes more

flexible when the thickness is reduced. An asphalt or cement treated open-graded permeable subbase, sufficient load transfer devices at joints, and tied concrete shoulder or widened outer lanes should be considered.

4. Further research is needed to address the effectiveness of load transfer across joints due to fiber reinforcement.

12. REFERENCES

1. Ramakrishnan, V., 1994, "Evaluation of Non-Metallic Fiber Reinforced Concrete in PCC Pavements and Structures," (SD94-04).

2. Ramakrishnan, V.,1993, "Quality Control and Evaluation of Fiber Reinforced Concrete," (SD87-02).

3. Ramakrishnan, V.; Oberling, G.; and Tatnall, P., 1987, "Flexural Fatigue strength of Steel Fiber Reinforced Concrete," Fiber Reinforced Concrete - Properties and Applications, American Concrete Institute Special Publication, SP-105, ACI, Detroit, pp.225-245.

4. Ramakrishnan, V.; Collapudi, S.; and Zeller, R., 1987, "Performance Characteristics and Fatigue Strength of Polypropylene Fiber Reinforced Concrete," Fiber Reinforced Concrete - Properties and Applications, ACI SP-105, American Concrete Institute, Detroit.

5. Ramakrishnan, V., 1985, "Flexural Fatigue Strength of Dramix Steel Fiber Reinforced Concrete," A report submitted to Bekaert Steel Wire Corporation, Nile, Illinois.

6. Ramakrishnan, V., and Coyle, W.V., 1983, "Steel Fiber Reinforced Superplasticized Concrete for Rehabilitation of Bridge Decks and Highway Pavements," report DOT/RSPA/DMA-50/84-2, Office of University Research, U.S. Department of Transportation.

7. "AASHO Interim Guide for the Design of Rigid Pavement Structure," Committee on Design, April 1962.

8. AASHTO, 1993, "AASHTO Guide for Design of Pavement Structures," American Association of State Highway and Transportation Officials, Washington D.C.

9. ACI Committee 544, 1988, "Design Considerations of Steel Fiber Reinforced Concrete," ACI Structural Journal, V. No.5, Sept.-Oct., pp. 563-580.

10. ACI Committee 544, 1984, "State-of-the-Art Report on Fiber Reinforced Concrete," ACI 544. 1R-82, Fiber Reinforced Concrete - International Symposium, SP-81, ACI, pp 411-431.

11. ACI Committee 544, 1984, "Guide For Specifying, Mixing, Placing, and Finishing Steel Fiber Reinforced Concrete," ACI 554.3R-84, Fiber Reinforced Concrete - International Symposium, SP-81, ACI, pp 441-450.

12. Clemmer, H. F., 1923, "Fatigue of concrete," Proceedings, ASTM, Vol. 22, II, pp. 408-419.

13. Darter, M. I., and E. J. Barenberg, 1977, "Design of Zero-Maintenance Plain Jointed Concrete Pavement,", Report No. FHWA-RD-77-111/112, Vol. I & II, Federal Highway Administration.

14. Ernest K. Schrader, 1984, "Design Methods for Pavements with Special Concretes," Fiber Reinforced Concrete - International Symposium, SP-81, ACI, pp 197-212.

15. Goldbeck, A. T., 1919. "Thickness of concrete Slabs," Public Roads, pp34-38.

16. Heinrichs, K. W., M. J. Liu, M. I. Darter, S. H. Carpenter, and A. M. Ioannides, 1989 "Rigid Pavement Analysis and Design," Report No. FHWA-RD-88-068, Federal Highway Administration.

17. Huang, Y. H., and S. T. Wang, 1973, "Finite Element Analysis of concrete Slabs and Its Implications for Rigid Pavement Design," Highway Research Record 466.

18. Huang, Y. H., 1974, "Finte Element Analysis of Slabs on Elastic Solids," Transportation Engineering Journal of ASCE, Vol. 100, No. TE28, pp. 403-416.

19. Huang, Yang H., 1993, "Pavement Analysis and Design," Prentice-Hall, Inc., Englewood Cliffs, New Jersey 07632.

20. Johnston, C. D., and Robert W. Zemp, 1991, " Flexural Fatigue Performance of Steel Fiber Reinforced Concrete - Influence of Fiber Content, Aspect Ratio, and Type", ACI Material Journal, July-August.

21. Nasser, H., 1988,"Performance Characteristics of Steel and Polypropylene Fiber Reinforced Concrete," M.S. Thesis, South Dakota School of Mines and Technology, Rapid City, SD.

22. Older, C., 1924. "Highway Research in Illinois," Transactions, ASCE, Vol.87, pp. 1180-1222.

23. Packard, R. G., and S. D. Tayabji, 1985, "New PCA Thickness Design Procedure for Concrete Highway and Street Pavements," Third International Conference on Concrete Pavement Design and Rehabilitation, Purdue University, pp. 225-236.

24. PCA, 1966, "Thickness Design for Concrete Pavements"

25. PCA, 1984, "Thickness Design for Highway and Street Pavements," Portland Cement Association, Skokie. Illinois 60077.

26. PCA, 1991, "Design and Construction of Joints for Concrete Highways," 1991, Concrete Paving Technology, Portland Cement Association, Skokie. Illinois 60077.
27. Parker, F., 1974, "Steel Fibrous Concrete for Airport Pavement Applications," Technical Report No. S-74-12, U.S. Army Engineer Waterways Experiment Station, Vicksburg.

28. Pickett, G., and S. Badaruddin, 1956, "Influence Chart for Bending of a Semi-infinite Pavement Slab," Proceedings, Ninth International Congress on Applied Mechanics, Vol. 6, pp. 396-402.

29. Robert G. Packard, and Gordon K. Ray, 1984 "Performance of Fiber-Reinforced Concrete Pavement," Fiber Reinforced Concrete - International Symposium, SP-81, ACI, pp 325-349.

30. SHRP, 1993, "Distress Identification Manual for the Long-Term Pavement Performance Project", SHRP-P-338, Strategic Highway Research Program, Washington, DC.

31. Schrader, E. K., and Lankard, D. R., Apr. 1983, "Inspection and Analysis of Curl in Steel Fiber Reinforced Concrete Pavement Applications," Bekaert Steel Wire Corp., Pittsburgh.

32. Smith, K. D. et al., 1990, "Performance of Jointed Concrete Pavements," Publication No. FHWA-RD-89-136 to 141, Vol. I to VI, Federal Highway Administration.

33. Smith, R. E., M. I. Darter, and S. M. Herrin, 1979, "Highway Pavement Distress Identification Manual for Highway Condition and Quality of Highway Construction Survey," Contract DOT-FH-11-9175/NCHRP 1-19, Federal Highway Administration.

34. Tabatabaie, A. M., 1977, "Structural Analysis of Concrete Pavement Joints," Ph.D. Thesis, University of Illinois.

35. Tabatabaie, A. M., and E. J. Barenberg, 1980, "Structural Analysis of Concrete Pavement Systems," Transportation Engineering Journal, ASCE, Vol. 106, No.TE5, pp. 493-506.

36. Tayabji, S. D. and B. E. Colley, 1986, "Analysis of Jointed concrete Pavement." Report No. FHWA-RD-86-041, Federal Highway Administration.

37. Westergaard, H. M., 1926, "Stresses in Concrete Pavements Computed by Theoretical Analysis," Pubic Roads, Vol. 7, pp. 25-35.

38. Gopalaratnam, Vellore, Surendra P Shah, Gordon B. Batson, Marvin E. Criswell, V. Ramakrishnan, and Methi Wecharatana, 1991, "Fracture Toughness of Fiber Reinforced Concrete", ACI Material Journal, V. 88, No. 4. July-August, pp. 339-353